Supporting Information

Design and Synthesize of a Weakly Solvated Electrolyte for High-Performance Fluoride-Ion Batteries

Jia Xiang[1, &], Wei Zou[2, &], Ying Lei[2, &], Hua-Jun Shawn Fan[2, *], Rongwen Lu[1, *], Shufen Zhang[1]

1 State Key Laboratory of Fine Chemicals, Frontiers Science Center for Smart Materials Oriented Chemical Engineering, Dalian University of Technology, Dalian 116024, P. R. China.

2 College of Chemistry Engineering, Sichuan University of Science and Engineering, Zigong 643000, P R China.

****Corresponding author. Email: lurw@dlut.edu.cn, fan27713@yahoo.com***

Table of Contents

A. Materials and Instrumentation

1. Materials

All compounds and solvents were sourced from reputable suppliers. Anhydrous-grade NMR solvents, specifically chloroform-d and dimethyl sulfoxide-d6, were obtained from Adamas-beta® Reagent Co., Ltd. Formic acid (>98%), 2,2-dimethylpropan-1-amine (99%), pivalaldehyde (>96%), palladium(II) acetate ($Pd(OAc)_2$; 98%), formaldehyde (36.5–38% in water), and tri-t-butylphosphine (10% in n-pentane) were procured from Aladdin's Reagent Co. Ethyl acetate (99.9%), *N*,*N*-dimethylformamide (DMF; >99.8%), *o*-xylene (>98%), ethanol (C_2H_5OH; >99%), methanol (CH_3OH; 99.9%), potassium hydroxide (KOH; 90%), and magnesium sulfate ($MgSO_4$; 98%) were sourced from Sinopharm Reagent Co. Additional reagents, including phenazine (>99%), sodium hydrosulfite ($Na_2S_2O_4$; >79%), sodium tert-butoxide (99%), sodium cyanoborohydride (95%), methyl iodide (CH_3I; >98%), acetonitrile (99.9%), silver(I) fluoride (AgF; >98%), 2-iodoanisole (98%), 4-iodoanisole (99%), 2-iodotoluene (>98%), 4-iodotoluene (>98%), 2,4-dimethoxybenzeneboronic acid (>98%), copper(I) iodide (CuI; 99.999%), copper(I) oxide (Cu_2O; >97%), *N*,*N*'-dimethylethylenediamine (DMEDA; >98%), and *N*,*N*-dimethyltrifluoroacetamide (DMTFA) were also obtained from Adamas-beta® Reagent Co., Ltd. Electronic-grade cerium(III) fluoride (CeF_3), cerium (Ce), and lithium fluoride (LiF) were procured from Sente Target Co. Carbon nanotubes were acquired from Chengdu Organic Chemistry Co., and poly(vinylidene fluoride) (PVDF; electronic grade) was supplied by Arkema.

2. Instrumentation

Scanning electron microscopy (SEM) was performed using a Thermo Scientific Apreo 2C microscope. For this analysis, the polymer powder was applied to conductive adhesive and coated with a thin (~2 nm) layer of gold (Au), similar to thin-film materials. Transmission electron microscopy (TEM) images were acquired using a Talos F200S microscope operating at 200 kV, with analytical characterization conducted via SUPERX-type spectroscopy. The negative electrode material was randomly sampled using a Thermo Scientific Helios 5 CX focused ion beam (FIB). The specific surface area of the polymeric materials was measured using a fully automated physical adsorption analyzer (Mack ASAP 2460, USA) employing the BET method. X-ray photoelectron spectroscopy (XPS) analysis was performed on a Thermo Fisher Scientific ALPHA spectrometer with high-resolution Al Kα X-rays as the excitation source. To minimize solvent interference, circulating electrode materials were depressurized to remove surface solvents and stored in an inert atmosphere. Binding energy calibration was referenced to the carbon 1s peak at 284.8 eV, and XPS peaks were deconvoluted and fitted using Avantage XPS software. Fourier-transform infrared (FTIR) spectra were recorded on a Frontier Near/Mid-IR Std device (Bruker

Optik GmbH, INVENIO R) with samples prepared as KBr pellets in an argon atmosphere. In-situ FTIR spectra of the batteries were acquired in an argon environment using a PerkinElmer Frontier, while in-situ electron paramagnetic resonance (EPR) measurements were conducted on a Bruker A300 spectrometer. Raman spectroscopy was performed using a Thermo Fisher Scientific DXR2xi system. Organic products were analyzed via ^{1}H, ^{13}C, and ^{19}F NMR on a Bruker 600 MHz NMR instrument. Laser confocal Raman spectroscopy was conducted with a Horiba Scientific LabRAM HR Evolution, utilizing a laser spot diameter of 2 μm, a power output of 1.5 mW, and an integration time of 30 seconds, all under an inert argon gas environment.

B. Synthetic Procedures

1. Synthesis of the imidazolium salt

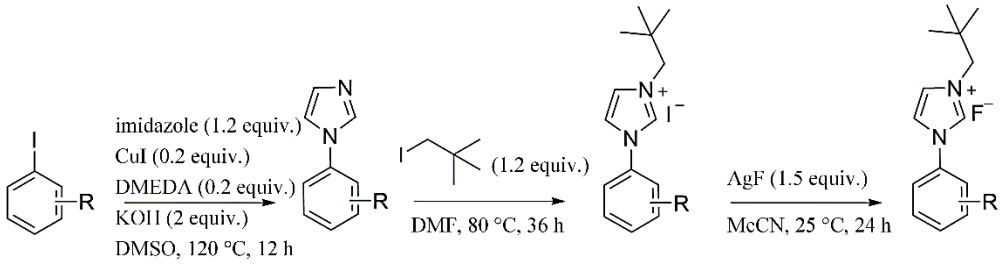

Figure S1. Synthesis process for phenylimidazole-based electrolyte.

Synthesis of phenylimidazole with reference to previously reported work.[1] To a three-necked flask, add benzene (1 mol, 1 equiv.) and imidazole (1.2 mol, 1.2 equiv.) sequentially. Purge the flask with nitrogen gas three times using a double-row tube. Then, add 2 L of dimethyl sulfoxide (DMSO), copper iodide (10 mmol, 10 mol%), *N*,*N*'-dimethylethylenediamine (DMEDA) (20 mmol, 20 mol%), and KOH (2 mol, 2.0 equiv.). The reaction mixture was stirred under nitrogen at 110 ℃ for 12 hours, and the progress was monitored by TLC. Upon completion, the mixture was allowed to cool to room temperature, followed by quenching with an excess of H_2O (10 equiv.). The polymer by-product was filtered off, and the filtrate was extracted with 100 × 3 mL of ethyl acetate. The organic phase was dried over anhydrous sodium sulfate, and the crude product was purified by preparative chromatography.

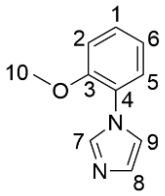

1-(2-methoxyphenyl)-1*H*-imidazole: Light yellow liquid, yield 73.4%. ^{1}H NMR (600 MHz,

Chloroform-*d*) δ 7.77 (t, *J* = 1.3 Hz, 1H, H-7), 7.34 (m, 1H, H-5), 7.26 (dd, *J* = 7.8, 1.7 Hz, 1H, H-2), 7.19 (t, *J* = 1.3 Hz, 1H, H-9), 7.15 (t, *J* = 1.3 Hz, 1H, H-8), 7.03 (m, 2H, H-1, 6), 3.82 (s, 3H, H-10); ^{13}C NMR (600 MHz, Chloroform-*d*) δ (128.83, C-1), (112.35, C-2), (152.60, C-3), (126.53, C-4), (121.02, C-5), (125.55, C-6), (137.83, C-7), (128.96, C-8), (120.28, C-9), (55.8, C-10).

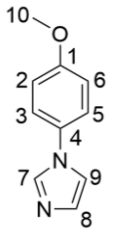

1-(4-methoxyphenyl)-1*H*-imidazole: Light yellow liquid, yield 70.5%. ^{1}H NMR (600 MHz, Chloroform-*d*) δ 7.76 (t, *J* = 1.1 Hz, 1H, H-7), 7.30(m, 2H, H-3, 5), 7.20 (t, *J* = 1.1 Hz, 1H, H-9), 7.18 (d, *J* = 1.1 Hz, 1H, H-8),6.98 (m, 2H, H-2, 6), 3.85 (s, 3H, H-10); ^{13}C NMR (600 MHz, Chloroform-*d*) δ (158.95, C-1), (114.91, C-2), (123.25, C-3), (130.07, C-4), (123.25, C-5), (114.91, C-6), (135.89, C-7), (130.74, C-8), (118.80, C-9), (55.63, C-10).

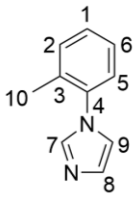

1-(*o*-tolyl)-1*H*-imidazole: Light yellow liquid, yield 70.2%. ^{1}H NMR (600 MHz, Chloroform-*d*) δ 7.56 (m, 1H, H-7), 7.32 (m, 2H, H-1,6), 7.26 (m, 1H, H-2), 7.20 (m, 1H, H-9), 7.18 (t, *J* = 1.1 Hz, 1H, H-8), 7.03 (m, 1H, H-5), 2.16 (s, 3H, H-10). ^{13}C NMR (600 MHz, Chloroform-*d*) δ (131.30, C-1), (136.66, C-2), (126.88, C-3), (137.51, C-4), (126.55, C-5), (128.81, C-6), (136.66, C-7), (129.38, C-8), (120.51, C-9), (17.65, C-10).

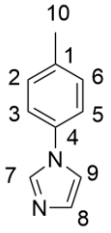

1-(*p*-tolyl)-1*H*-imidazole: Light yellow liquid, yield 75.8%. ^{1}H NMR (600 MHz, Chloroform-*d*) δ 7.81 (t, *J* = 1.1 Hz, 1H, H-7), 7.26 (s, 4H, H-2, 3, 5, 6), 7.24 (t, *J* = 1.1 Hz, 1H, H-9), 7.18 (t, *J* =

1.1 Hz, 1H, H-8), 2.39 (s, 3H, H-10). ^{13}C NMR (600 MHz, Chloroform-*d*) δ (137.49, C-1), (130.38, C-2), (121.47, C-3), (135.01, C-4), (121.47, C-5), (130.38, C-6), (135.65, C-7), (130.20, C-8), (118.83, C-9), (20.98, C-10).

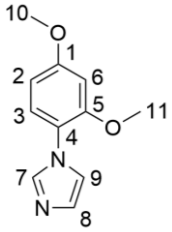

1-(2,4-dimethoxyphenyl)-1*H*-imidazole: Light yellow liquid, yield 46.3%. ^{1}H NMR (600 MHz, Chloroform-*d*) δ 7.67 (t, *J* = 1.2 Hz, 1H, H-7), 7.17 (d, *J* = 8.6 Hz, 1H, H-3), 7.14 (t, *J* = 1.2 Hz, 1H, H-9), 7.11 (t, *J* = 1.2 Hz, 1H, H-8), 6.58 (d, *J* = 2.6 Hz, 1H, H-6), 6.52 (dd, *J* = 8.6, 2.6 Hz, 1H, H-2), 3.84 (s, 3H, H-11), 3.80 (s, 3H, H-10). ^{13}C NMR (600 MHz, Chloroform-*d*) δ (160.35, C-1), (104.41, C-2), (128.56, C-3), (119.92, C-4), (153.87, C-5), (99.73, C-6), (137.90, C-7), (126.42, C-8), (120.60, C-9), (55.74, C-10), (55.59, C-10).

Iodized salt: In a 20 mL high-pressure reaction bottle, add the five imidazole derivatives synthesized in the previous step (1 mmol, 1 equiv.). Add 2 mL of DMSO as the solvent and stir for 10 minutes under a nitrogen atmosphere. Next, add homemade 1-bromo-2,2-dimethylpropane (2.2 mmol, 2.2 equiv.) and a catalytic amount of KI (0.05 mmol). The reaction was carried out at 130 ℃ for 24 hours. After completion, the solvent was removed by evaporation, and the product was purified by preparative chromatography.

Fluoride salt: Silver fluoride (AgF; 1.3 mmol, 1.3 equiv.) was added to a Schlenk flask, which was then evacuated and heated for 30 minutes. After cooling to room temperature, 50 mL of anhydrous acetonitrile was added, followed by the iodide synthesized in the previous step (1 mmol, 1 equiv.). The reaction vessel was covered with aluminum foil and left in the dark for 3 hours. The particles were then removed using a microporous membrane, and the filtrate was collected. The product was placed in an electrolyzer with platinum electrodes for both the positive and negative electrodes and subjected to a voltage of 3 V for 5 days. Afterward, the particles were filtered using a 0.22 μm membrane, and the filtrate was collected. The excess solvent was removed under anhydrous conditions. All steps were performed inside a receiving box, and this purification method was applied to all five imidazolyl quaternary ammonium salts.

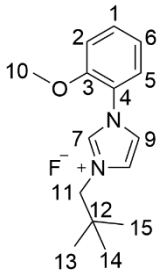

1-(2-methoxyphenyl)-3-neopentyl-1*H*-imidazolium fluoride: Transparent solid, yield 33.4%. ^{1}H NMR (600 MHz, DMSO-*d6*) δ 9,87 (s, 1H, H-7), 7.64 (dd, *J* = 3 Hz, 1H, H-5), 7.15 (qd, *J* = 3, 1.7 Hz, 2H, H-2, 6), 7.71 (t, *J* =6 Hz, 1H, H-9), 7.67 (t, *J* = 3 Hz, 1H, H-8), 7.53 (m, *J* = 3 Hz, 1H, H-1), 3.95 (s, 3H, H-10), 4.44 (s, 2H, H-11), 1.09 (s, 9H, H-13, 14, 15). ^{13}C NMR (600 MHz, DMSO-*d6*) δ (131.94, C-1), (112.78, C-2), (151.93, C-3), (122.68, C-4), (125.53, C-5), (123.03, C-6), (137.27, C-7), (123.78, C-8), (122.68, C-9), (56.57,C-10), (60.85, C-11), (32.53, C-12), (27.03, C-13, 14, 15). ^{19}F NMR (600 MHz, DMSO-*d6*) δ (70.36, 1F).

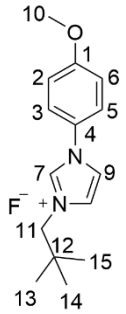

1-(4-methoxyphenyl)-3-neopentyl-1*H*-imidazolium fluoride: Transparent solid, yield 35.2%. ^{1}H NMR (600 MHz, DMSO-*d6*) δ 10.19 (t, *J* = 3Hz, 1H, H-7), 7.07 (d, *J* = 3Hz, 2H, H-2, 6), 7.77 (m, 2H, H-3, 5), 7.96 (t, *J* = 6, 6 Hz, 1H, H-9), 3.86 (s, 3H, H-10), 4.38 (s, 2H, H-11), 1.08 (s, 9H, H-13, 14, 15). ^{13}C NMR (600 MHz, DMSO-*d6*) δ (160.54, C-1), (115.35, C-2, 6), (124.81, C-3, 5), (127.20, C-4), (134.86, C-7), 124.81, C-8), (120.97, C-9), (55.78, C-10), (60.73, C-11), (32.31, C-12), (27.00, C-13, 14, 15). ^{19}F NMR (600 MHz, DMSO-*d6*) δ (72.64, 1F)

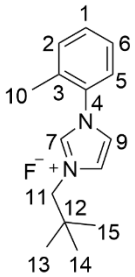

3-neopentyl-1-(*o*-tolyl)-1*H*-imidazolium fluoride: Transparent solid, yield 40.5%. ^{1}H NMR(600

MHz, DMSO-*d6*) δ 8.04 (t, *J* = 3 Hz, 1H, H-1), 7.56 (t, *J* = 3 Hz 2H, H-2, 6), 7.48 (td, *J* = 10 Hz, 1H, H-5), 9.63 (t, *J* = 3 Hz, 1H, H-7), 8.04 (t, *J* = 3 Hz, 1H, H-8), 8.12 (t, *J* = 3 Hz, 1H, H-9), 2.24 (s, 3H, H-10), 4.17 (s, 2H, H-11), 1.00 (s, 9H, H-13, 14, 15). ^{13}C NMR (600 MHz, DMSO-*d6*) δ (127.30, C-1), (124.60, C-2), (135.50, C-3), (124.60, C-4), (124.60, C-5), (123.62, C-6), (160.87, C-7), (120.69, C-8), (115.51, C-9), (31.63, C-10), (60.73, C-11), (32.31, C-12), (27.00, C-13, 14, 15). ^{19}F NMR (600 MHz, DMSO-*d6*) δ (72.63, 1F).

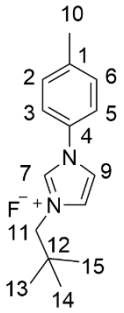

3-neopentyl-1-(*p*-tolyl)-1*H*-imidazolium fluoride: Transparent solid, yield 23.5%. ^{1}H NMR (600 MHz, DMSO-*d6*) δ 7.70 (m, 2H, H-2, 6), 7.48 (d, *J* = 12 Hz, 2H, H-3, 5), 9.8 (s, 1H, H-7), 7.97 (t, *J* = 3 Hz 1H, H-8), 8.33 (t, *J* = 3 Hz, 1H, H-9), 4.1 (s, 2H, H-11), 12 (s, 3H, H-12), 0.99 (s, 9H, H-13, 14, 15). ^{13}C NMR (600 MHz, DMSO-*d6*) δ (140.13, C-1), (130.90, C-2, 6), (122.31, C-3, 5), (132.85, C-4), (136.02, C-7), (125.22, C-8), (121.38, C-9), (21.06, C-10), (60.55, C-11), (32.46, C-12), (27.26, C-13, 14, 15). ^{19}F NMR (600 MHz, DMSO-*d6*) δ (72.59, 1F).

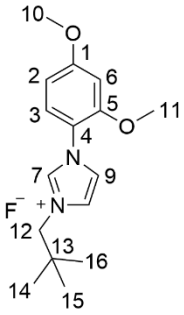

1-(2,4-dimethoxyphenyl)-3-neopentyl-1*H*-imidazolium fluoride: Light yellow transparent solid, yield 23.6%. ^{1}H NMR (600 MHz, DMSO-*d6*) δ 6.88 (d, *J* = 3 Hz, 1H, H-2), 7.57 (d, *J* = 10 Hz, 1H, H-3), 6.75 (dd, *J* = 3 Hz, 1H, H-6), 9.50 (t, *J* = 1.5 Hz, 1H, H-7), 7.92 (t, *J* = 3 Hz, 1H, H-8), 8.0 (t, J = 3 Hz, 1H, H-9), 3.86 (s, 3H, H-10), 3.97 (s, 3H, H-11), 4.11 (s, 2H, H-12), 0.97 (s, 9H, H-14, 15, 16). ^{13}C NMR (600 MHz, DMSO-*d6*) δ (153.99, C-1), (106.13, C-2), (138.33, C-3), (117.15, C-4), (162.30, C-5), (100.26, C-6), (127.73, C-7), (124.16, C-8), (124.08, C-9), (57.10, C-10), (56.49, C-11), (60.26, C-12), (32.53, C-13), (27.18, C-14, 15, 16). ^{19}F NMR (600 MHz, DMSO-*d6*) δ (70.15, 1F).

2. synthesis of trimethylneopentylammonium fluoride

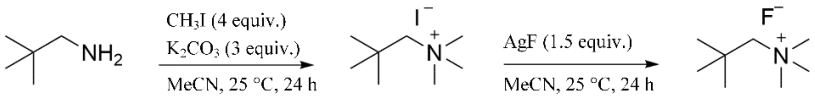

Figure S2. Synthesis process for Trimethylneopentylammonium fluoride.

Trimethylneopentylammonium fluoride: A three-necked flask was used to synthesize the compound. Neopentylamine (11.7 mL, 100 mmol) was added to the flask, followed by anhydrous K_2CO_3 (41.5 g, 300 mmol), CH_3I (24.91 mL, 400 mmol), and 500 mL of CH_3CN. The reaction mixture was heated to 40 °C, protected from light, and maintained at this temperature for 24 hours. After the reaction, the filtrate was obtained by filtration, and the solvent was removed by vacuum distillation to yield the crude product. The final product was purified by recrystallization using a 1:1 mixture of ethyl acetate and ethanol.

Silver fluoride (AgF; 1.3 mmol, 1.3 equiv.) was added to a Schlenk flask, which was evacuated and heated for 30 minutes. After cooling to room temperature, 50 mL of anhydrous acetonitrile was added, followed by the iodide synthesized in the previous step (1 mmol, 1 equiv.). The reaction vessel was covered with aluminum foil and left in the dark for 3 hours. The particles were removed using a microporous membrane, and the filtrate was collected. The product was then placed in an electrolyzer with platinum electrodes for both the positive and negative electrodes and subjected to a voltage of 3 V for 5 days. Afterward, the particles were filtered using a 0.22 μm membrane, and the filtrate was collected. The excess solvent was removed under anhydrous conditions.White solid, yield 73.3%. ^{1}H NMR (600 MHz, CD_3CN-*d3*) δ 3.28 (s, 2H), 3.15 (s, 9H), 1.13 (s, 9H). ^{13}C NMR (600 MHz, CD_3CN-*d3*) δ (77.02), (55.04), (33.36), (29.73). ^{19}F NMR (600 MHz, CD_3CN-*d3*) δ (72.24, 1F).

3. Synthesis of dimethyldineopentylammonium fluoride

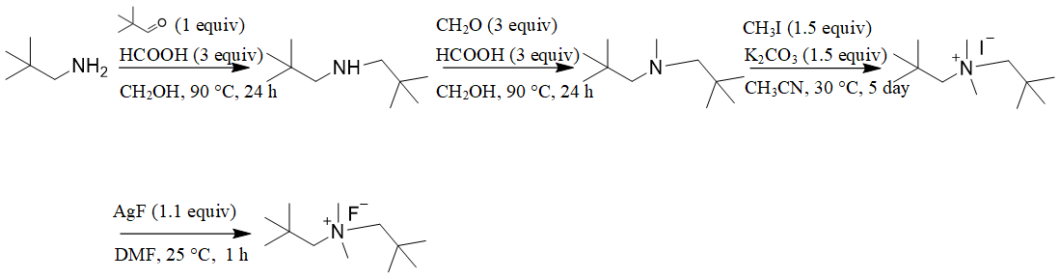

Figure S3. Synthesis process for dimethyldineopentylammonium fluoride.

Dineopentylamine: The method here refers to a previously published article.[2] A three-necked flask was employed to synthesize dineopentylamine. Neopentylamine (11.7 mL, 100 mmol) was

added to the flask, followed by the sequential addition of anhydrous magnesium sulfate (14 g, 100 mmol), neopentylaldehyde (12.1 mL, 110 mmol), and 100 mL of methanol. Formic acid (11.32 mL, 300 mmol) was then added dropwise to the reaction mixture. The temperature was increased to 80 °C, and the mixture was maintained at this temperature for 20 hours. After cooling to room temperature, a 1 M NaOH solution was added gradually until the pH reached ~8. The aqueous layer was extracted three times with 100 mL of ethyl acetate. The organic phase was separated, dried over anhydrous magnesium sulfate, and concentrated under reduced pressure. The final product was purified by recrystallization using a 1:1 mixture of ethyl acetate and hexane. White solid, yield 95%. m.p. 46 °C; ^{1}H NMR (400 MHz, Chlorform-*d*) δ: 2.82 (s, 4H), 1.09 (s, 18H); ^{13}C NMR (400 MHz, Chlorform-*d*) δ: 61.25, 31.18, 27.54.

***N*,2,2-trimethyl-*N*-neopentylpropan-1-amine:** Dineopentylamine (5.58 g, 36 mmol) was added to the reaction flask, followed by the addition of a 37% aqueous formaldehyde solution (17.5 mL, 216 mmol) and formic acid (5 mL, 216 mmol). After these reagents were combined, 100 mL of methanol was introduced, and the temperature of the mixture was increased to 80 °C. Thin-layer chromatography (TLC), using alkaline potassium permanganate as the color developer, was employed to monitor the reaction progress. The reaction was considered complete when the starting material was no longer detectable. To neutralize the excess formic acid, a 1 M NaOH solution was added gradually. After neutralization, the solvent was removed by evaporation under reduced pressure. The residue was then diluted with 100 mL of deionized water and extracted with 100 mL of ethyl acetate, repeating the extraction three times. The organic phase was isolated, dried over anhydrous magnesium sulfate, and concentrated by evaporation to yield the crude product. The crude product was further purified by flash column chromatography. Colorless clear liquid, yield 70%. b.p. 180 °C; ^{1}H NMR (400 MHz, Chlorform-*d*) δ: 2.32 (s, 3H), 2.21 (s, 4H), 0.90 (s, 18H); ^{13}C NMR (400 MHz, Chlorform-*d*) δ: 74.56, 48.13, 33.39, 28.81.

Dimethyldineopentylammonium iodine: A 100 mL three-necked flask was used for the synthesis. N,2,2-Trimethyl-N-neopentylpropan-1-amine (2.34 mL, 20 mmol) and iodomethane (1.87 mL, 30 mmol) were added to the flask, followed by 50 mL of DMF. The reaction was carried out at room temperature, shielded from light, for 5 days. After this period, the solvents were removed by distillation under reduced pressure, yielding a white crude product. The crude product was recrystallized using a 5:1 mixture of ethyl acetate and methanol. Following recrystallization, the product was filtered and washed with ethyl acetate. The final product was dried in a vacuum oven at 40 °C for 12 hours.

Dimethyldineopentylammonium fluoride: Inside a glove box, 20 mL of purified, de-watered acetonitrile was added to a 50 mL polytetrafluoroethylene (PTFE) reaction flask. A solution containing silver fluoride (AgF; 1.40 g, 11 mmol) and an iodide salt (3.13 g, 10 mmol) was then introduced. The mixture was stirred at room temperature for 2 hours. After this period, solid materials were removed using a needle filter, and the filtered mixture was transferred to an electrolytic bath. The mixture underwent decomposition at 3 V for 5 days, aiming to remove silver ions and residual water. Finally, the solvent was removed by distillation under reduced pressure, all under inert gas protection. The resultant product was maintained in the glove box for storage. White solid, yield 45%. ^{1}H NMR (400 MHz, CD_3CN-*d3*) δ: 2.32 (s, 4H), 2.31 (s, 6H), 0.9 (s, 18H); ^{13}C NMR (600 MHz, CD_3CN-*d3*) δ (72.11), (47.99), (31.82), (27.47). ^{19}F NMR (600 MHz, CD_3CN-*d3*) ^{19}F NMR (400 MHz, CD_3CN-*d3*) δ: 72.18 (s, 1F).

4. Synthesis of the cathode electrode material of the dihydrophenazinebased polymer (p-TPPZ)

The method here refers to a previously published article.[3] Phenazine (6 g, 33.3 mmol) was placed in a three-necked flask, evacuated, and then dissolved in 150 mL of ethanol. The solution was purged with argon for 15 minutes and stirred slowly for 30 minutes. Sodium dithionite (58 g, 333 mmol) was dissolved in 300 mL of water and slowly added to the system. The reaction mixture was purged with argon for an additional 10 minutes, and the temperature was raised to 80 °C. The mixture was refluxed for 12 hours. The light green product was washed several times with deionized water. The crude product was then dispersed in 300 mL of anhydrous ethanol, heated and stirred, and purified by recrystallization. Finally, the product was dried in a vacuum oven at 80 °C for 12 hours to obtain 5,10-dihydrophenazine, which was stored under an inert atmosphere for further use.

5,10-Dihydrophenazine (2.18 g, 12 mmol), 1,3,5-tribromobenzene (2.83 g, 12 mmol), palladium acetate (54 mg, 0.24 mmol), and sodium tert-butoxide (2.88 g, 30 mmol) were placed in a Schlenk flask and evacuated three times with argon. Next, 120 mL of *o*-xylene was added, and the mixture was purged with argon for 15 minutes while stirring vigorously. Tri-tert-butylphosphine (116 μL, 0.48 mmol) was then added. The mixture was heated at 120 °C for 12 hours. After cooling to room temperature, the resulting solid was filtered off and purified using a Soxhlet extractor with a sequence of deionized water, methanol, toluene, and diethyl carbonate. Finally, the product was dried in a vacuum oven at 70 °C for 12 hours.

5. Electrode sheet preparation

Electron-grade hydrogenated nitrile butadiene rubber (HNBR) was used as the binder for the

cathode, while electron-grade polyvinylidene fluoride (PVDF) was used for the anode. The cathode mixture, consisting of p-TPPZ (active material), carbon nanotubes, and HNBR, was prepared in a weight ratio of 4:2:0.5 (active material: carbon nanotubes: HNBR). The anode mixture, consisting of CeF_3 (active material), carbon nanotubes, and PVDF, was prepared in a weight ratio of 4:0.5:0.5 (active material: carbon nanotubes: PVDF). Both mixtures were homogenized in an inert atmosphere using a ball mill and stirred with anhydrous DMF as the solvent. The resulting pastes were applied to the current collectors inside a glove box using a spatula and then dried under vacuum at 100 °C for 12 hours. After drying, the materials were pressed into 14 mm diameter discs using a tablet press. The anode was prepared by coating a copper foil current collector with the CeF_3 slurry, while a gold foil current collector was used for the cathode.

All experimental procedures and material handling were conducted under strict anhydrous and anaerobic conditions. To ensure the complete removal of adsorbed moisture, all glassware and CR2025 coin cell components were pre-dried in a vacuum oven at 100°C for 8 hours. Solvents were dried by standard methods until the residual water content was reduced to below 1 ppm (detection limit), as confirmed by coulometric titration. The materials were then transferred via airbag to an argon-filled glove box, maintaining an inert environment with O_2 and H_2O levels below 0.1 ppm.

6. Accumulation of buffer phases on negative electrode sheets by RF sputtering

The electrode interface protection strategy described previously was employed. The anode electrode plate was affixed to a 10×10 cm, 5 mm thick stainless steel plate using conductive adhesive. The pressure was then reduced to 1 mTorr under vacuum, followed by the injection of argon to stabilize the pressure at 9 mTorr. The electrode was first activated with plasma, and after 10 minutes, a robotic arm positioned the activated electrode directly opposite the RF sputtering source. During this process, a nanometer-thick LiF layer was deposited on the electrode surface as an inert protective coating.

7. Electrochemical measurements

The electrode materials used in this study were p-TPPZ (cathode) and $LiF–CeF_3$ (anode), as prepared in the previous section. These materials were assembled in an argon-filled glove box with extremely low levels of water ($H_2O < 0.01$ ppm) and oxygen ($O_2 < 0.1$ ppm). The electrolyte was selected from a range of pre-prepared fluoride salts and formulated as a 1 M fluoride ion solution using BTFE/DMTFA (1:1) solvent synthesized in-house. Prior to use, the electrolyte's water content was rigorously measured using Karl Fischer titration to ensure it did not exceed 1

ppm. If this criterion was not met, further purification was performed. System testing was conducted using a CHI760E electrochemical workstation (Chenhua, Shanghai, China) and a Wuhan LAND battery testing system at 25 °C.

All three-electrode system cells used a titanium mesh as the counter electrode and Ag/AgCl as the reference electrode. Linear sweep voltammetry (LSV) was conducted on a CHI760E electrochemical workstation (Shanghai Chenhua) at a scan rate of 1 mV s^{-1}, with 0.5 mL of electrolyte added to the three-electrode system, and a voltage range from -2.0 V to 4.0 V. The working electrode consisted of a PVDF paste coated onto stainless steel. Constant current charge-discharge (GCD) measurements of the p-TPPZ||LiF–CeF_3 cell were performed at 25°C using the Wuhan LAND cell testing system. Electrochemical impedance spectroscopy (EIS) was carried out using a Tatsunhua electrochemical workstation, with a measurement frequency range from 100 kHz to 0.01 Hz. EIS data were used to determine the impedance of the p-TPPZ||LiF–CeF_3 cell and to calculate the ionic diffusion coefficient (D) (**Equations 1** and **2**) and activation energy barrier (Ea). To calculate E_a, the charge transfer resistance (R_{ct}) of the p-TPPZ||LiF–CeF_3 cell was measured at temperatures ranging from 5°C to 45°C, with the open-circuit voltage recorded. The activation energy barrier (Ea) was then calculated using the Arrhenius equation (**Equation 3**). The ionic conductivity of the electrode materials at different temperatures was determined using **Equation 4**.

$$\mathrm{D} = \frac{1}{2}\frac{(RT)^2}{(nACσF^2)^2} \tag{1}$$

$$Z' = R_s + R_{ct} + \sigma_w \omega^{-0.5} \tag{2}$$

Where R is the universal gas constant, T is the absolute temperature (in kelvin), A is the electrode area, n is the number of transferred electrons, F is the Faraday constant, C is the F^- concentration, Q is the Warburg coefficient, and ω is the angular frequency.

$$\frac{1}{R_{ct}} = A \exp\left(\frac{-Ea}{RT}\right) \tag{3}$$

Where R is the universal gas constant, T is the absolute temperature (in kelvin), R_{ct} is the charge transfer resistance.

$$\acute{O} = \frac{1}{R_{ct}}\frac{L}{S} \tag{4}$$

Where Ó is ionic conductivity, L is thickness of electrode material, and S is Area of electrode material.

C. Theoretical calculation

Theoretical calculations were conducted using Gaussian software, specifically the Gaussian16 package. Density Functional Theory (DFT) calculations were performed with the

B3LYP functional and the 6-311+G(d) basis set. Grimme's DFT-D3 methodology was employed to account for dispersion interactions among all atoms in the adsorption models. A convergence criterion of 1×10^{-8} eV was applied to ensure calculation accuracy. The Multiwfn program, combined with VMD, was utilized for calculating and visualizing molecular orbitals, Fukui functions, and electrostatic potential (ESP) maps.

D. Figure Captions

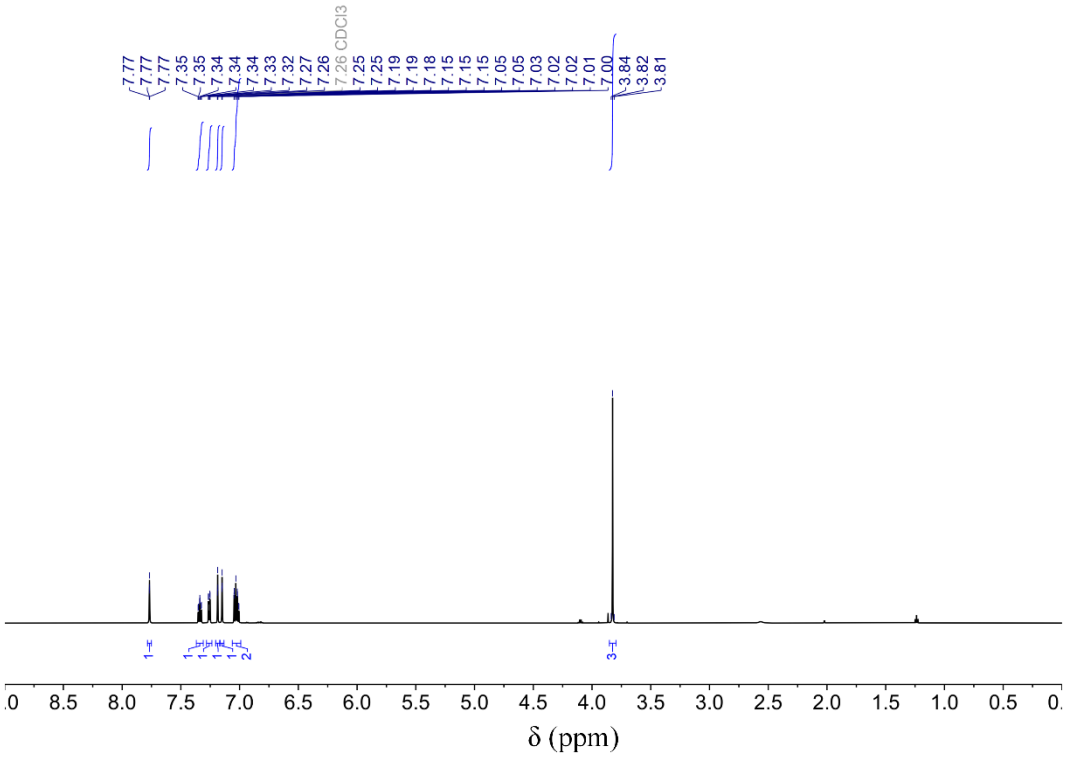

Figure S4. ^{1}H NMR of 1-(2-methoxyphenyl)-1*H*-imidazole

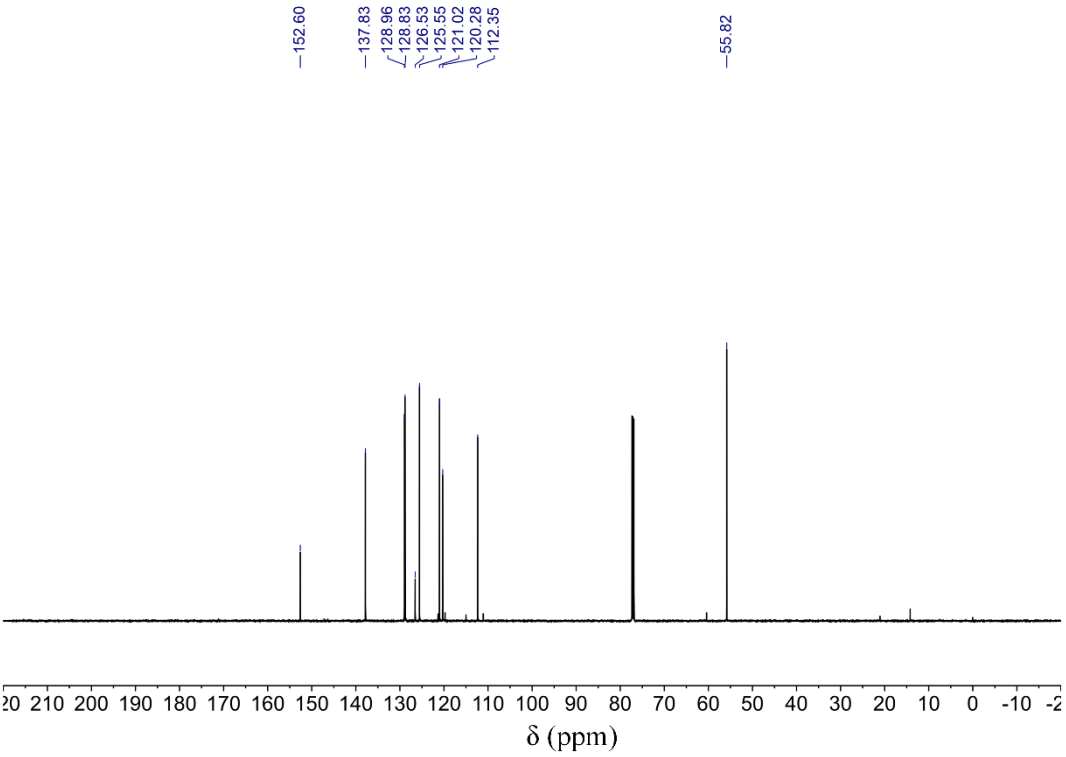

Figure S5. ^{13}C NMR of 1-(2-methoxyphenyl)-1*H*-imidazole

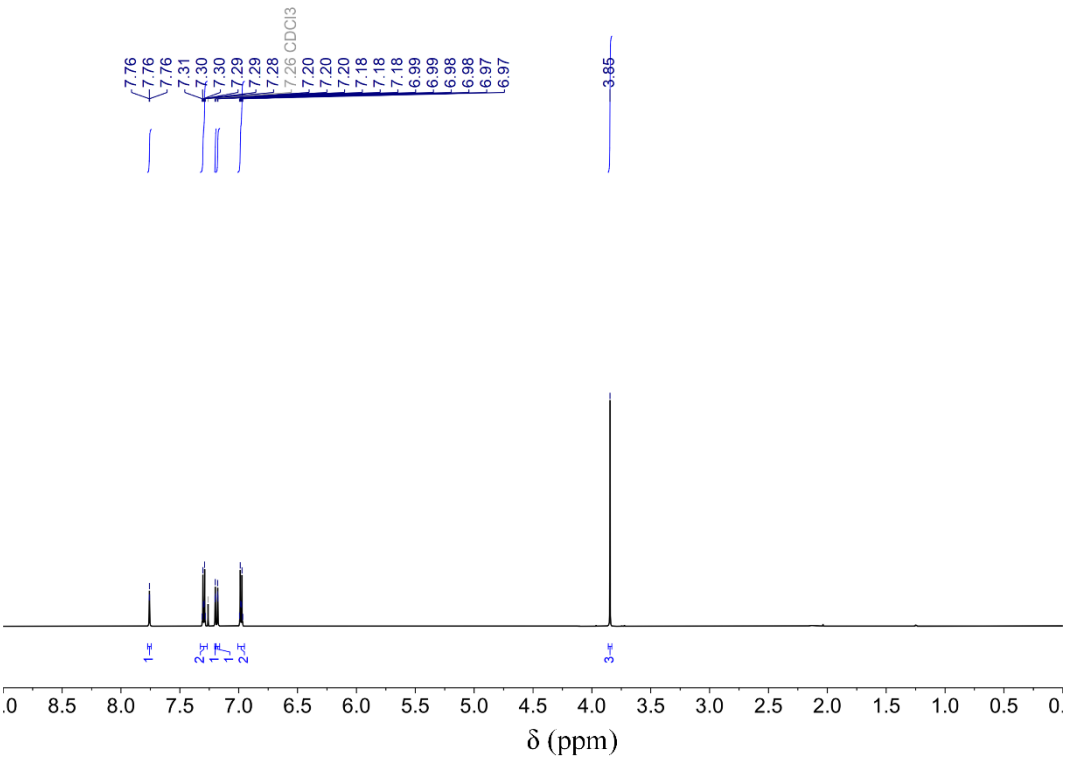

Figure S6. ^{1}H NMR of 1-(4-methoxyphenyl)-1*H*-imidazole

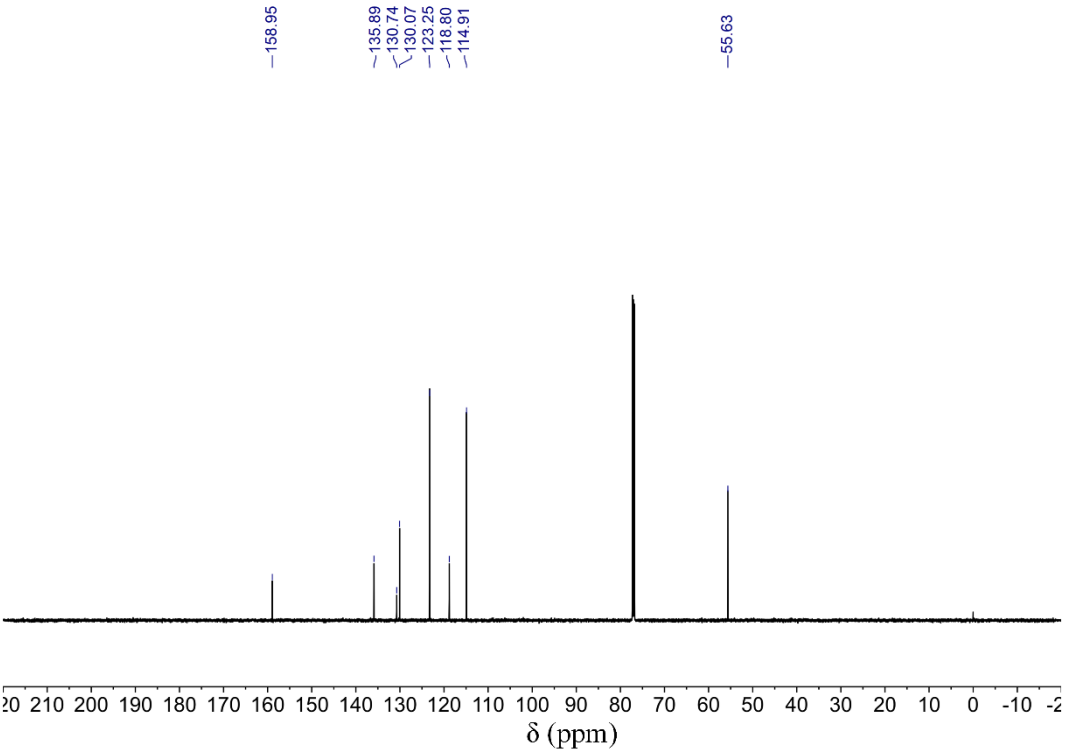

Figure S7. ^{13}C NMR of 1-(4-methoxyphenyl)-1*H*-imidazole

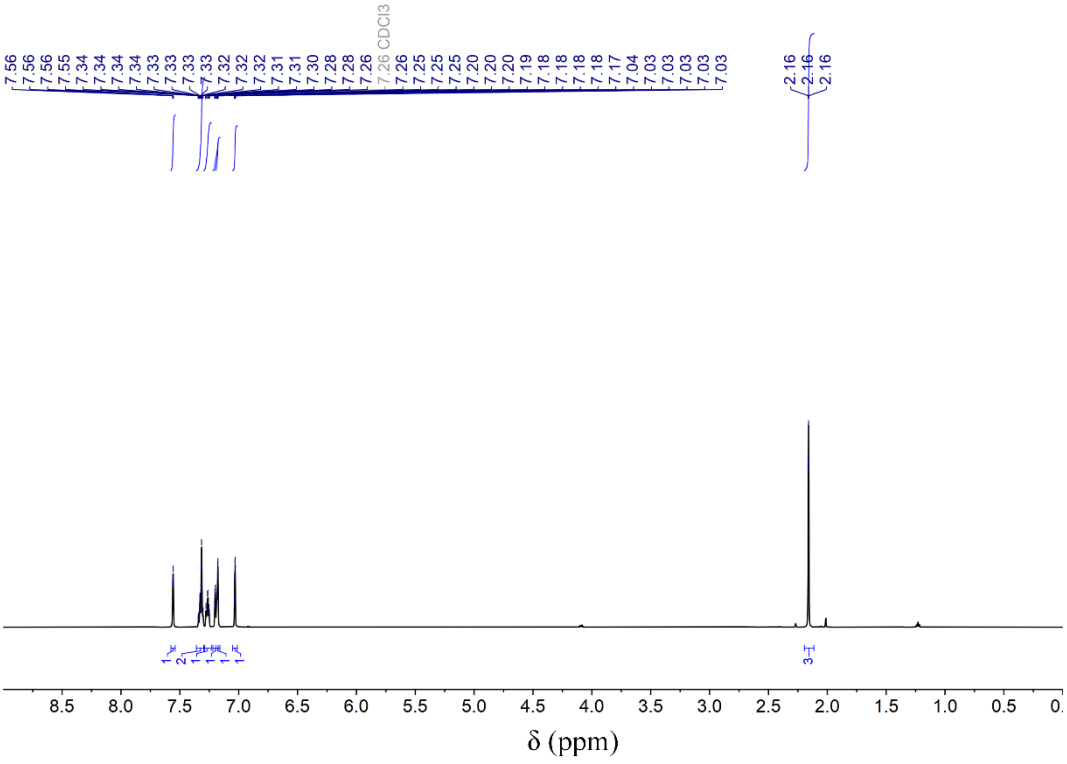

Figure S8. ^{1}H NMR of 1-(*o*-tolyl)-1*H*-imidazole

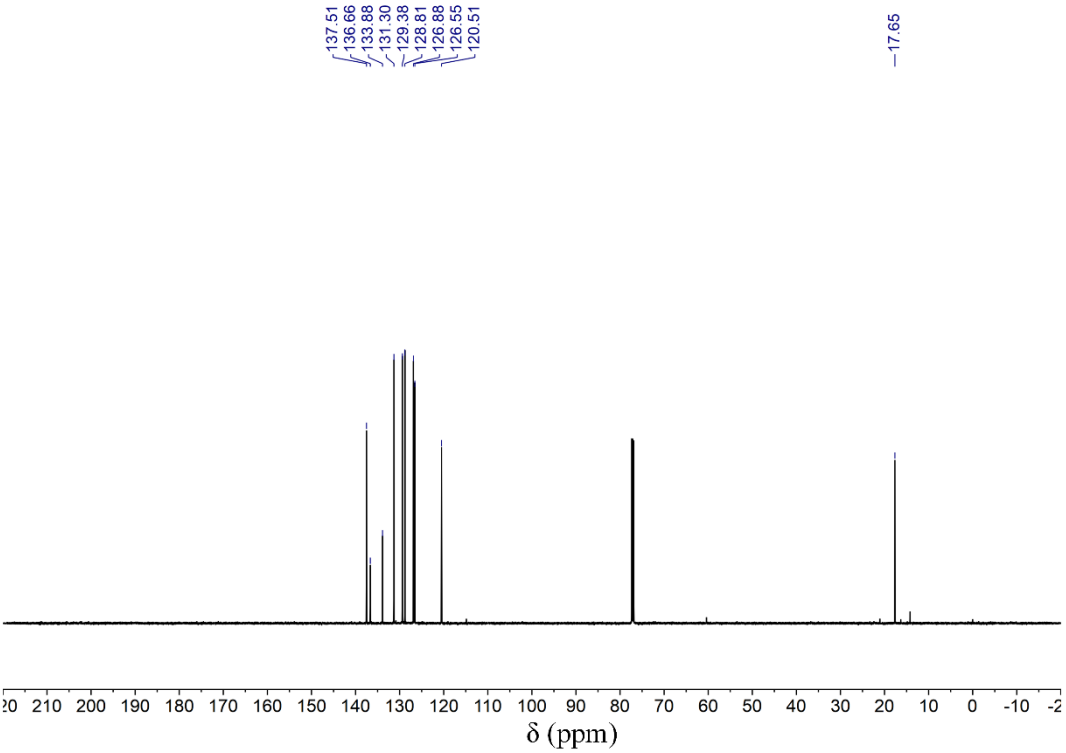

Figure S9. ^{13}C NMR of 1-(*o*-tolyl)-1*H*-imidazole

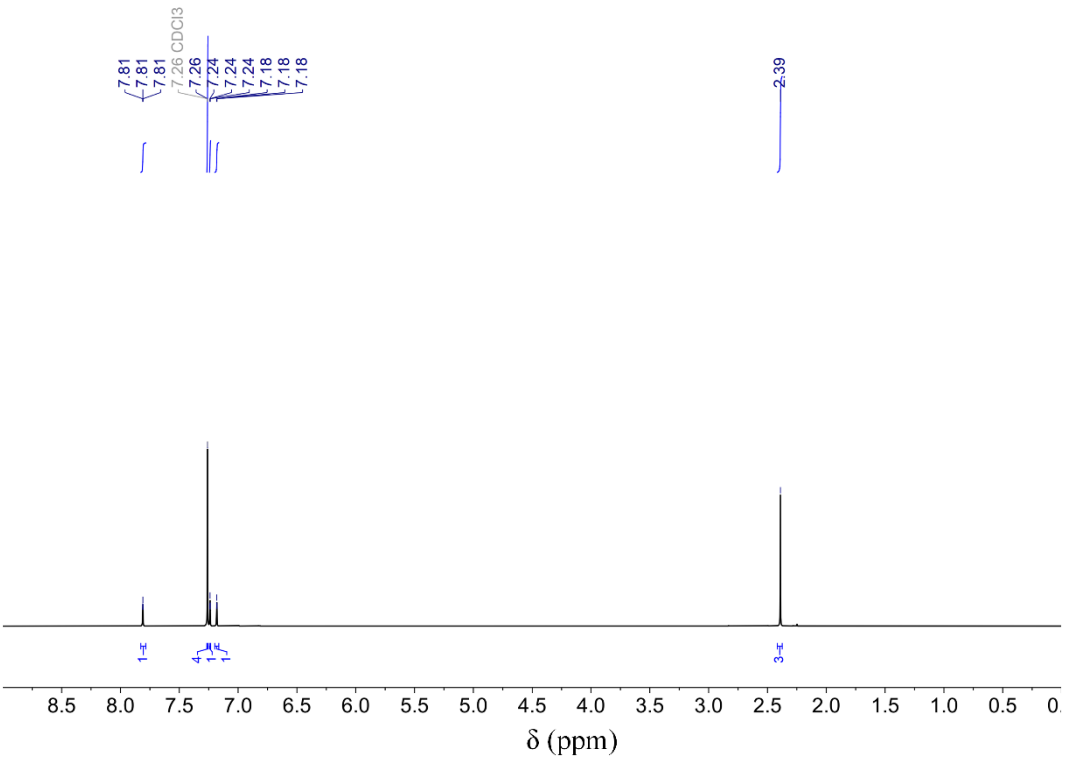

Figure S10. ^{1}H NMR of 1-(*p*-tolyl)-1*H*-imidazole

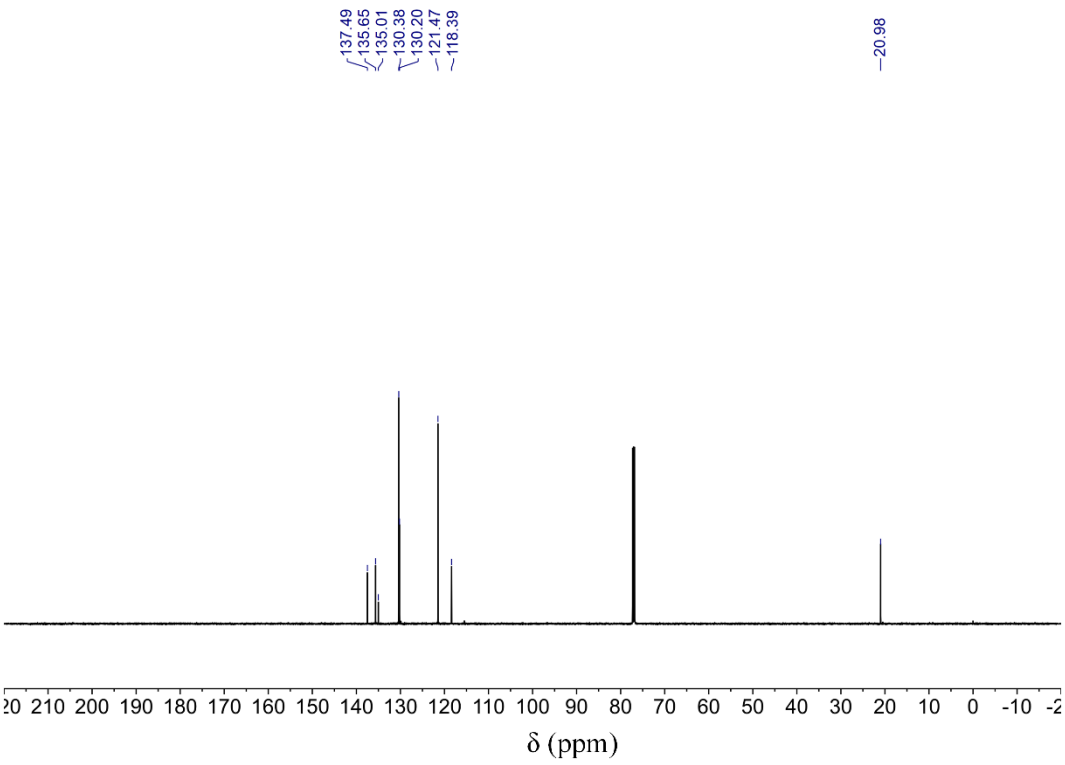

Figure S11. ^{13}C NMR 1-(*p*-tolyl)-1*H*-imidazole

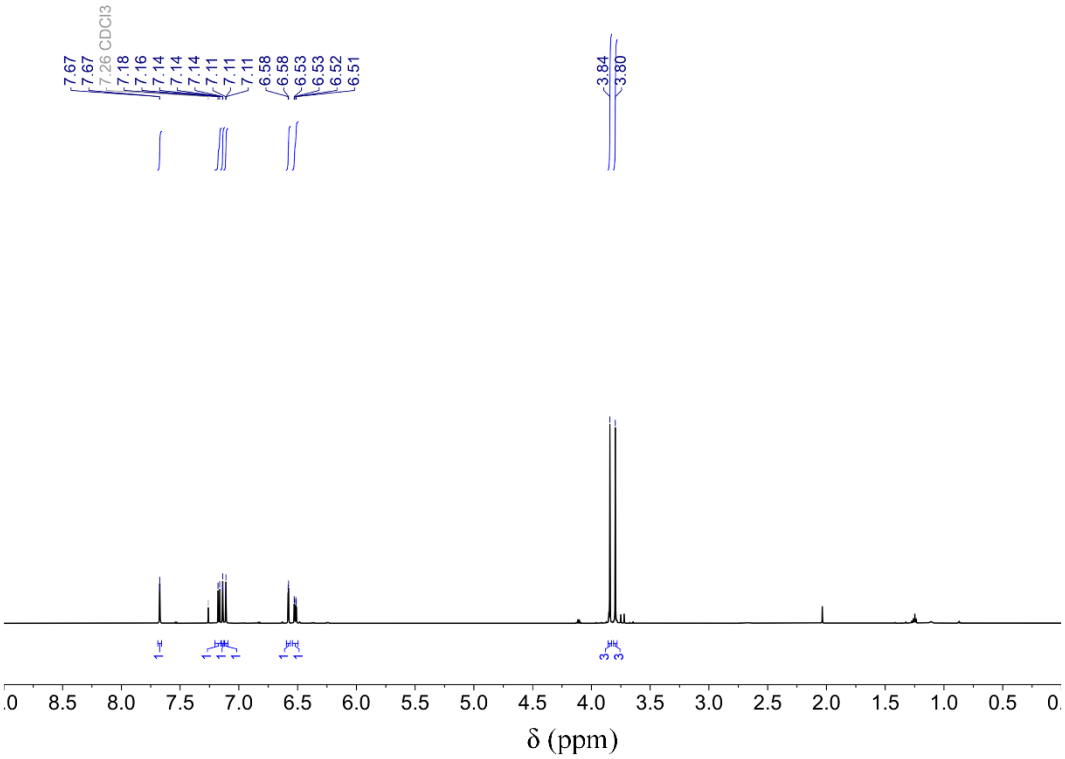

Figure S12. ^{1}H NMR of 1-(2,4-dimethoxyphenyl)-1*H*-imidazole

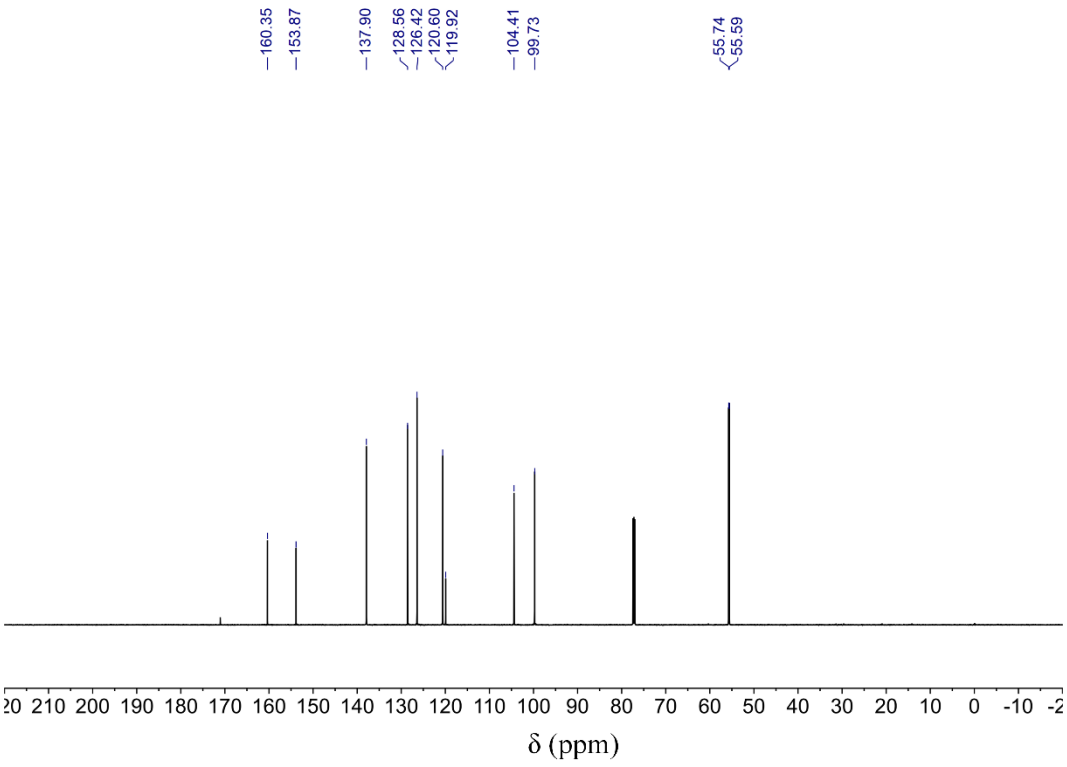

Figure S13. ^{13}C NMR of 1-(2,4-dimethoxyphenyl)-1*H*-imidazole

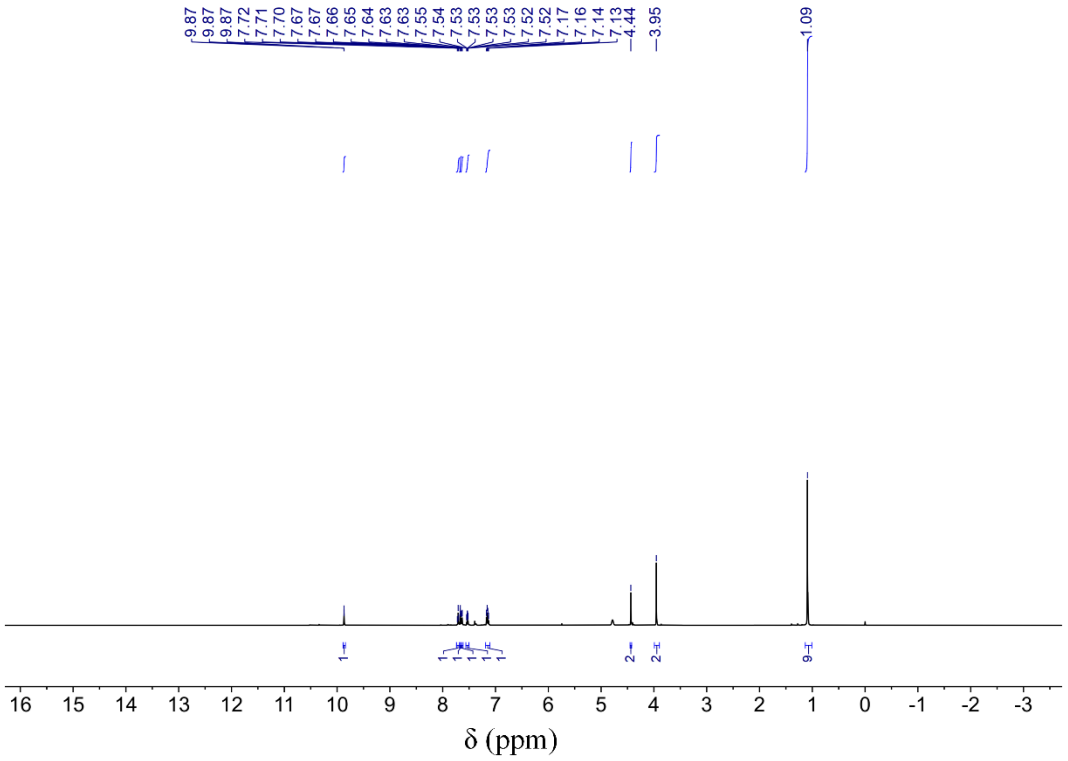

Figure S14. ^{1}H NMR of 1-(2-methoxyphenyl)-3-neopentyl-1*H*-imidazolium fluoride

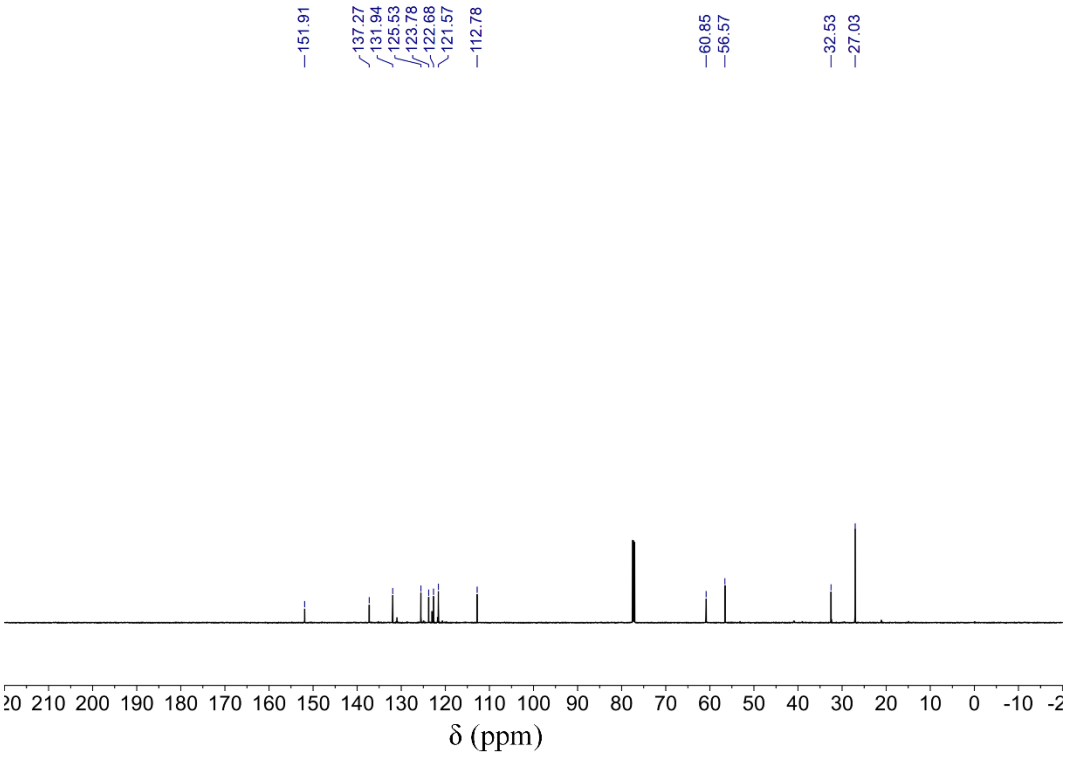

Figure S15. ^{13}C NMR of 1-(2-methoxyphenyl)-3-neopentyl-1*H*-imidazolium fluoride

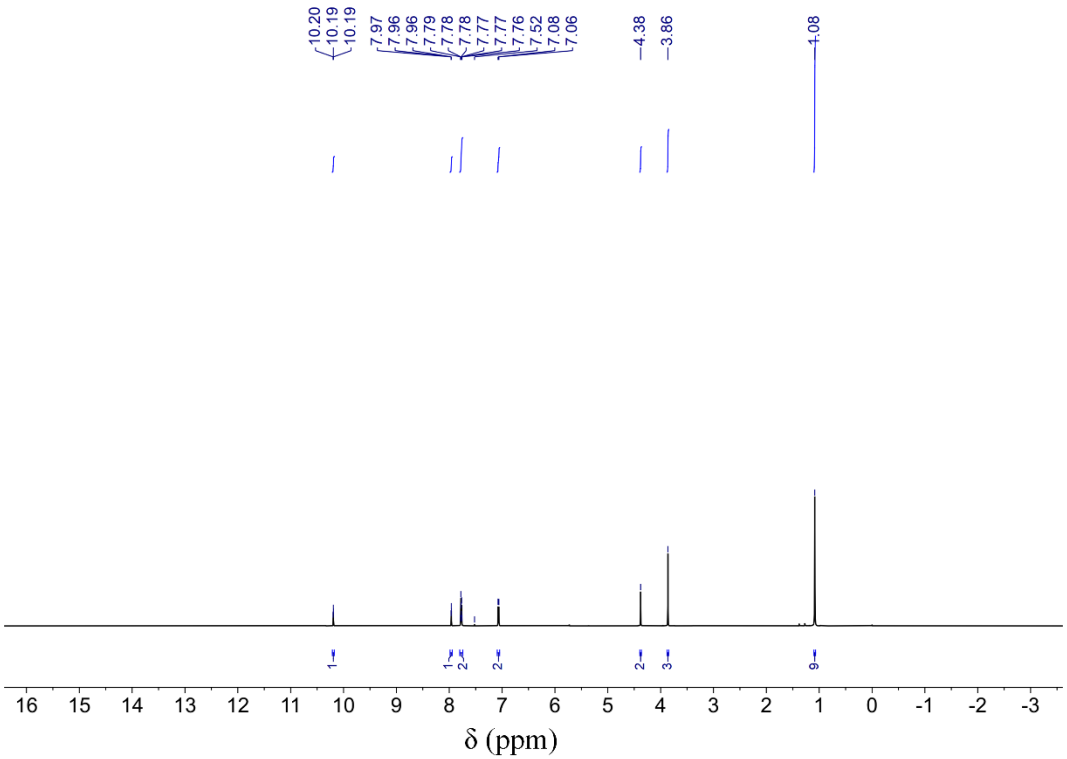

Figure S16. ^{1}H NMR of 1-(4-methoxyphenyl)-3-neopentyl-1*H*-imidazolium fluoride

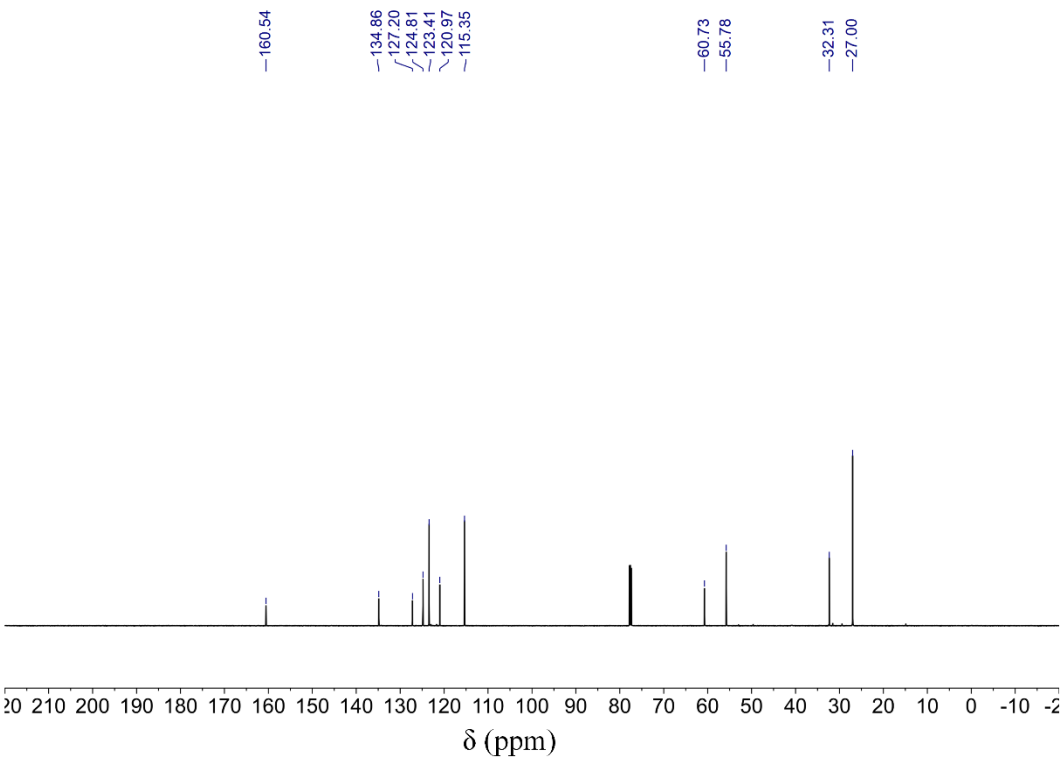

Figure S17. ^{13}C NMR of 1-(4-methoxyphenyl)-3-neopentyl-1*H*-imidazolium fluoride

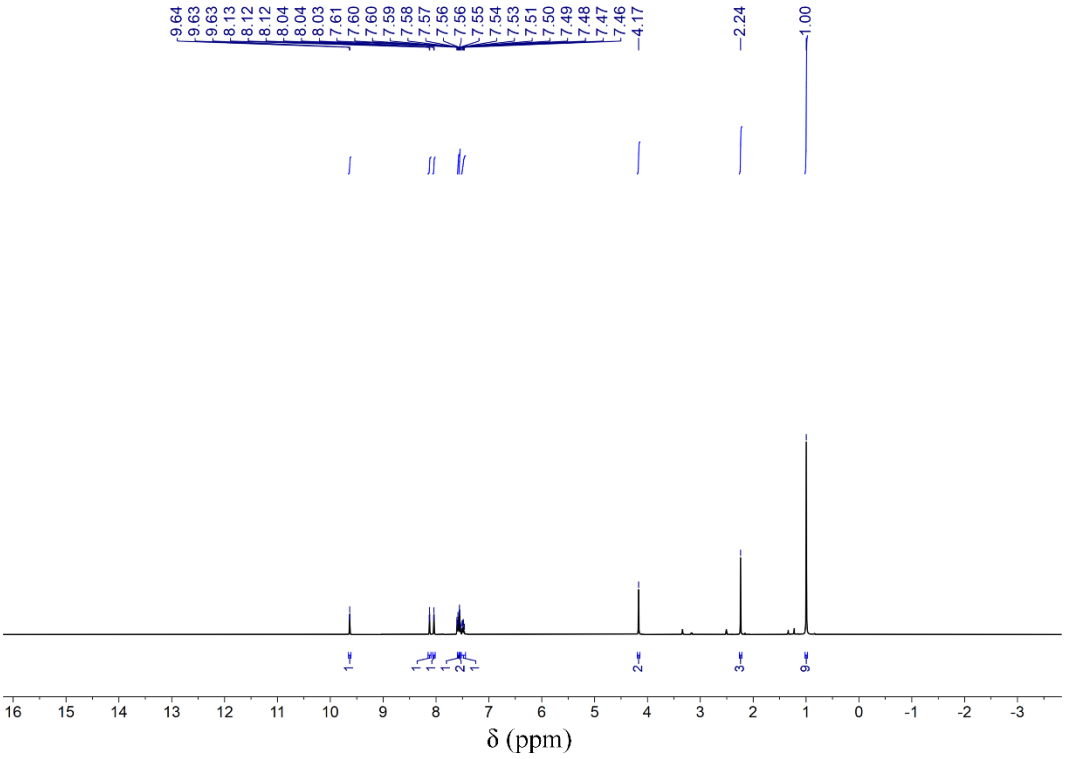

Figure S18. ^{1}H NMR of 3-neopentyl-1-(*o*-tolyl)-1*H*-imidazolium fluoride

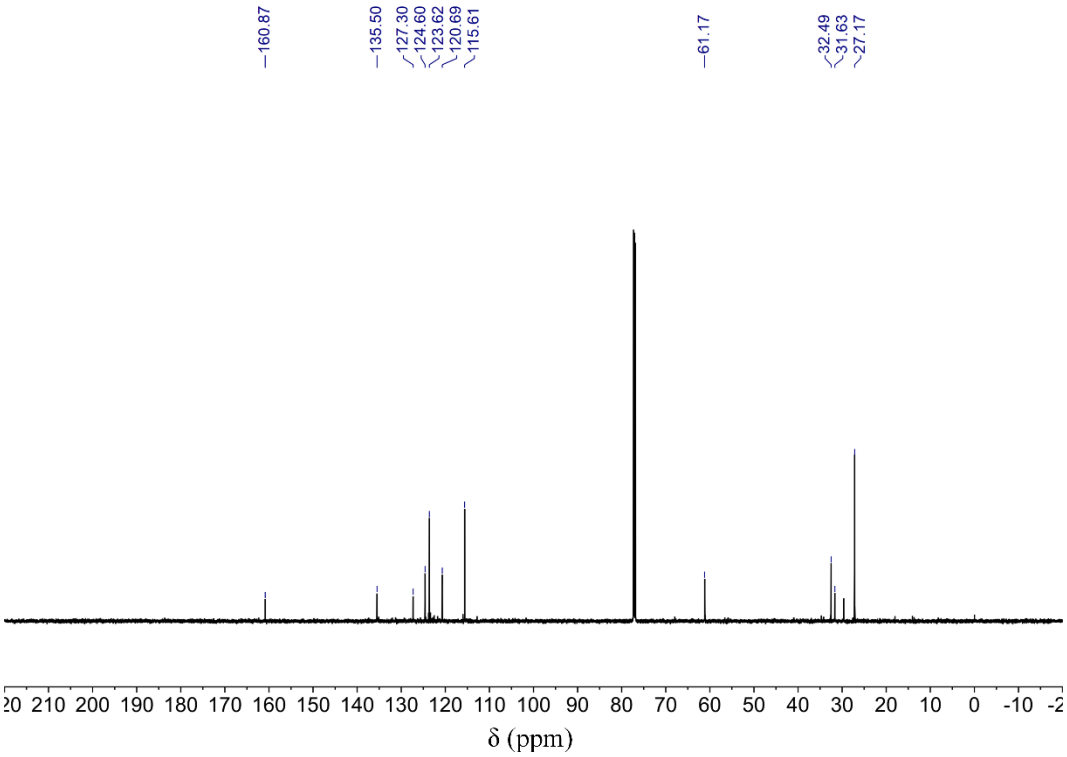

Figure S19. ^{13}C NMR of 3-neopentyl-1-(*o*-tolyl)-1*H*-imidazolium fluoride

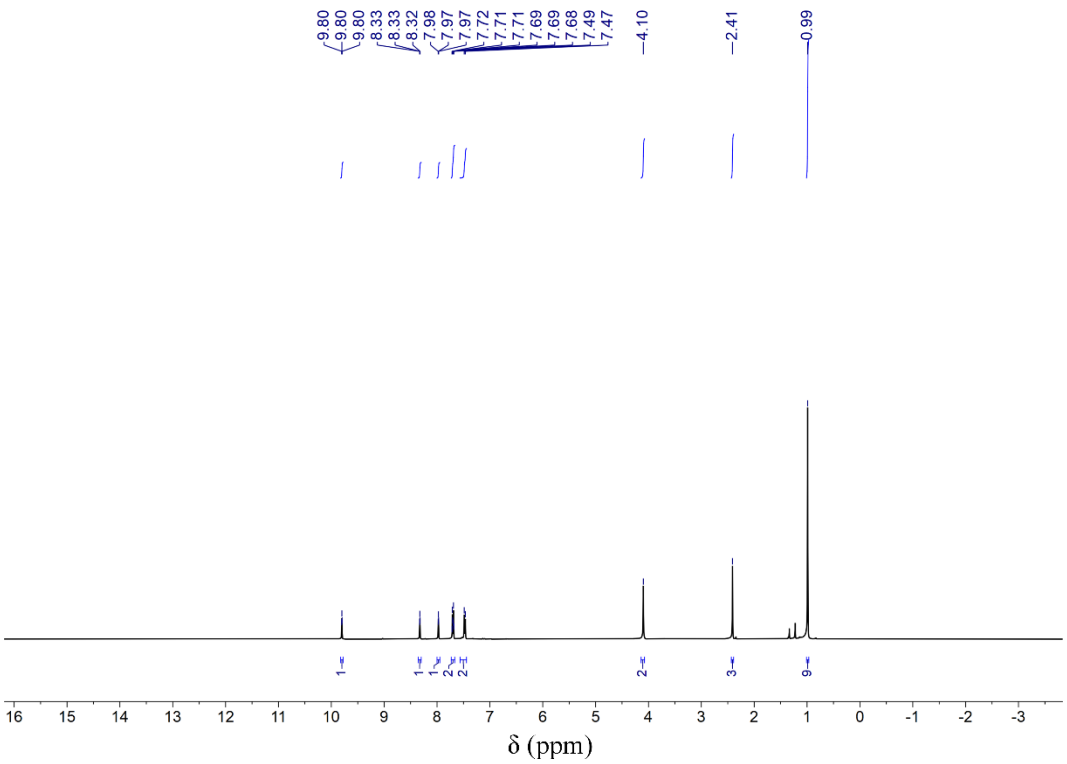

Figure S20. ^{1}H NMR of 3-neopentyl-1-(*p*-tolyl)-1*H*-imidazolium fluoride

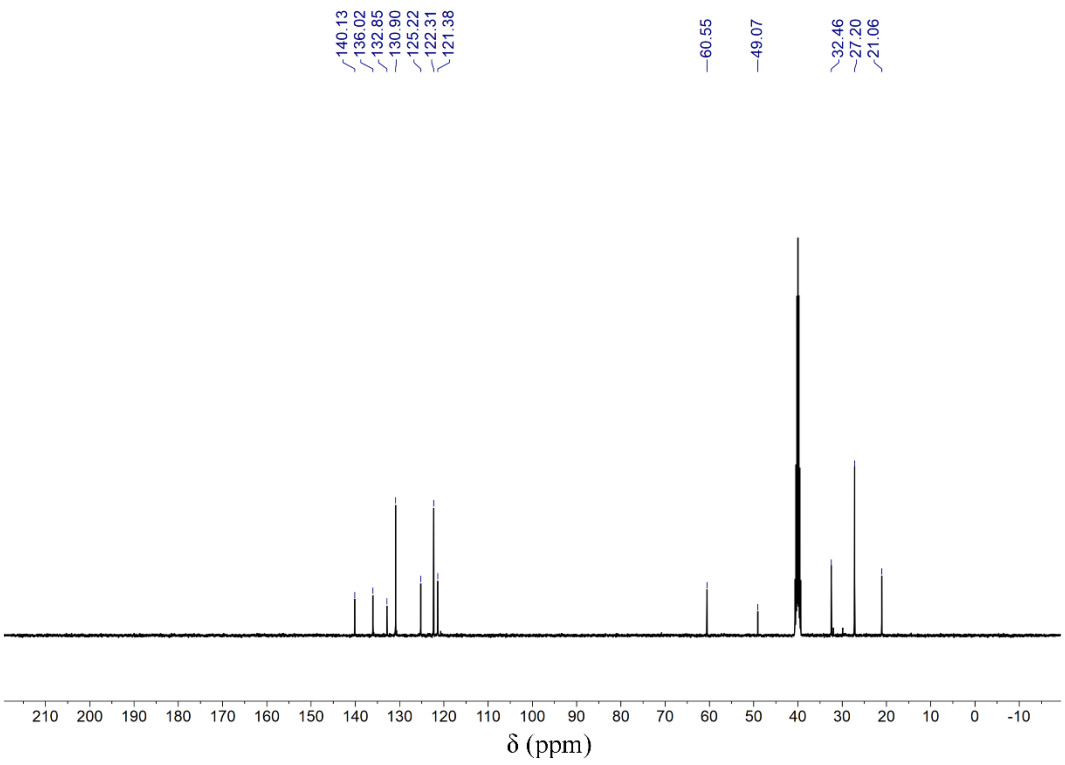

Figure S21. ^{13}C NMR of 3-neopentyl-1-(*p*-tolyl)-1*H*-imidazolium fluoride

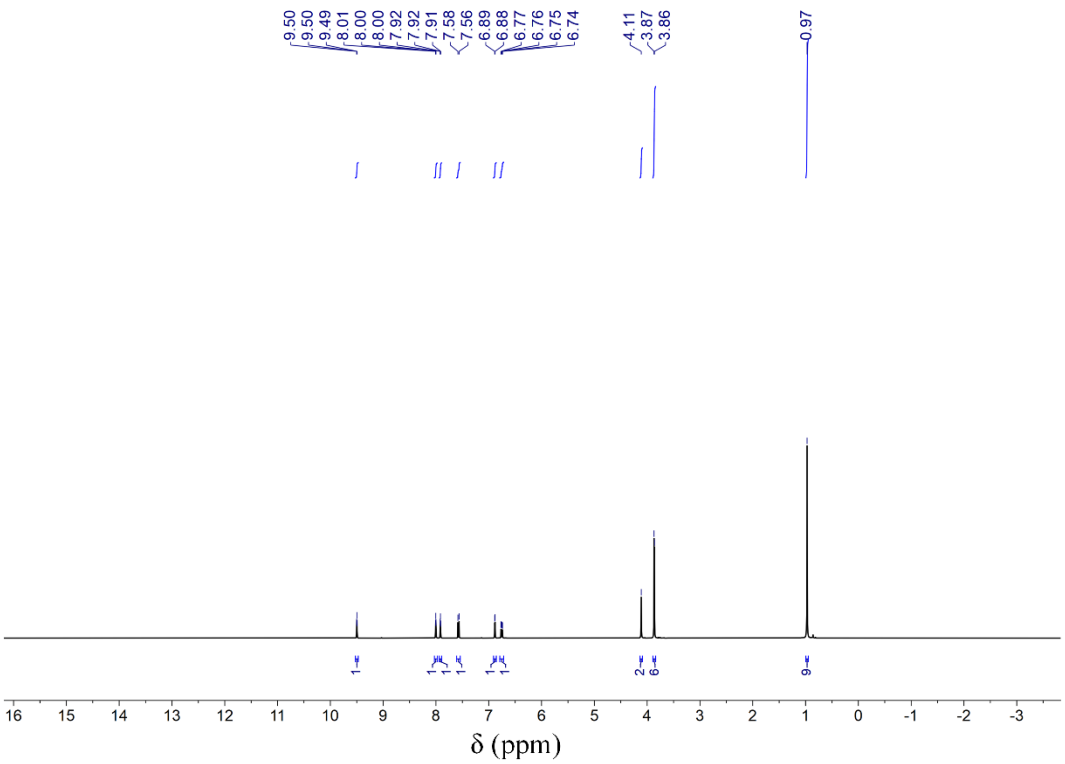

Figure S22. ^{1}H NMR of 1-(2,4-dimethoxyphenyl)-3-neopentyl-1*H*-imidazolium fluoride

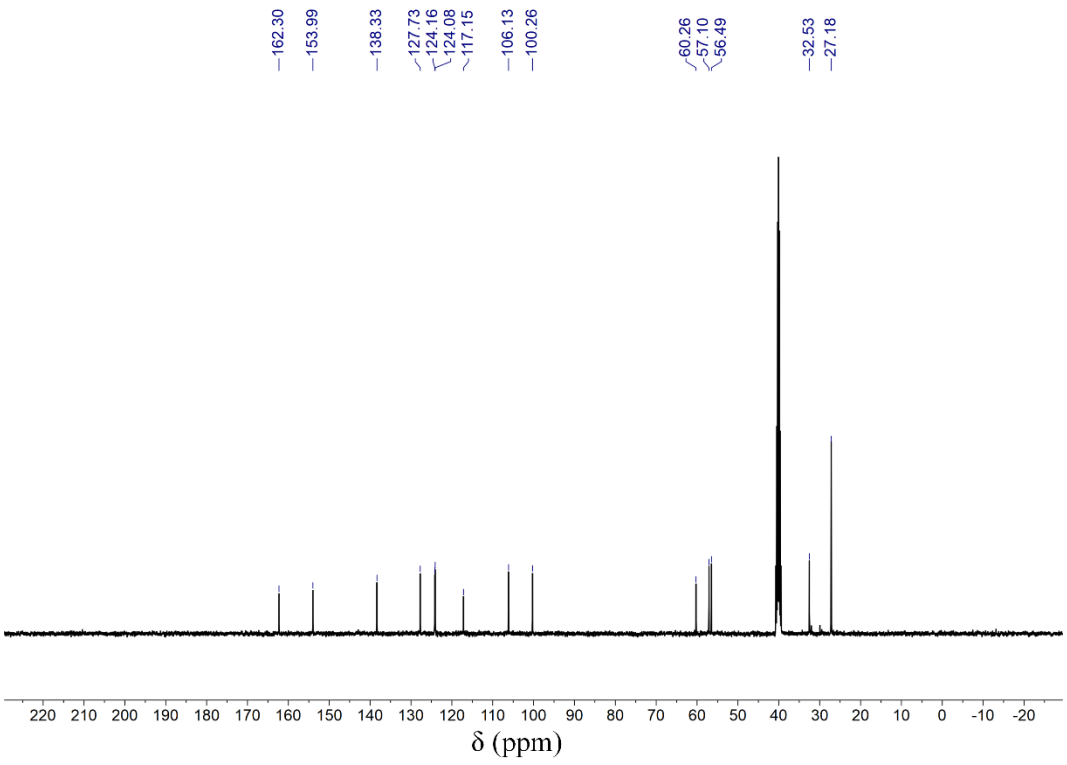

Figure S23. ^{13}C NMR of 1-(2,4-dimethoxyphenyl)-3-neopentyl-1*H*-imidazolium fluoride

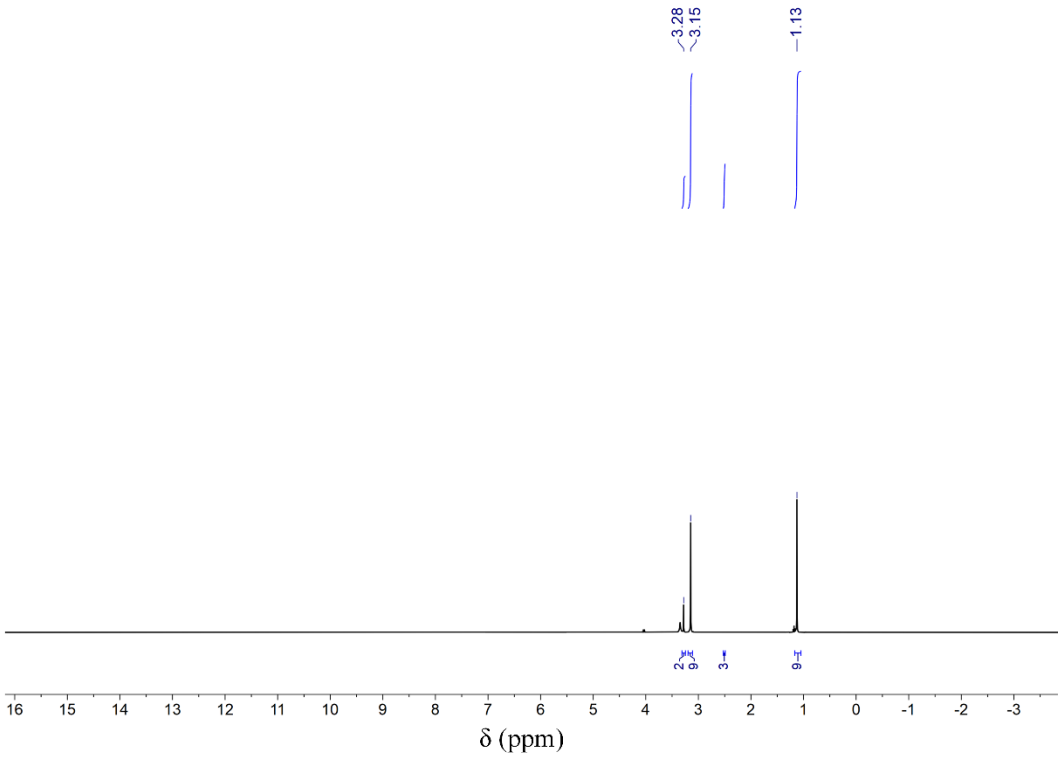

Figure S24. ^{1}H NMR of Trimethylneopentylammonium fluoride

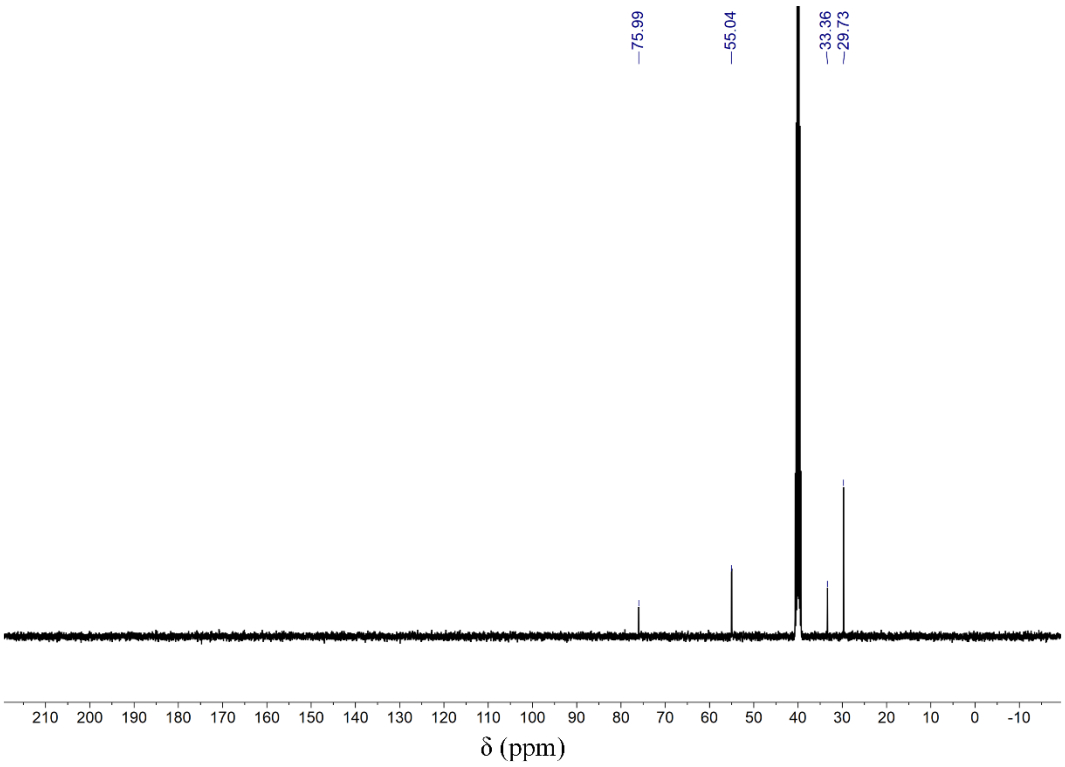

Figure S25. ^{13}C NMR of Trimethylneopentylammonium fluoride

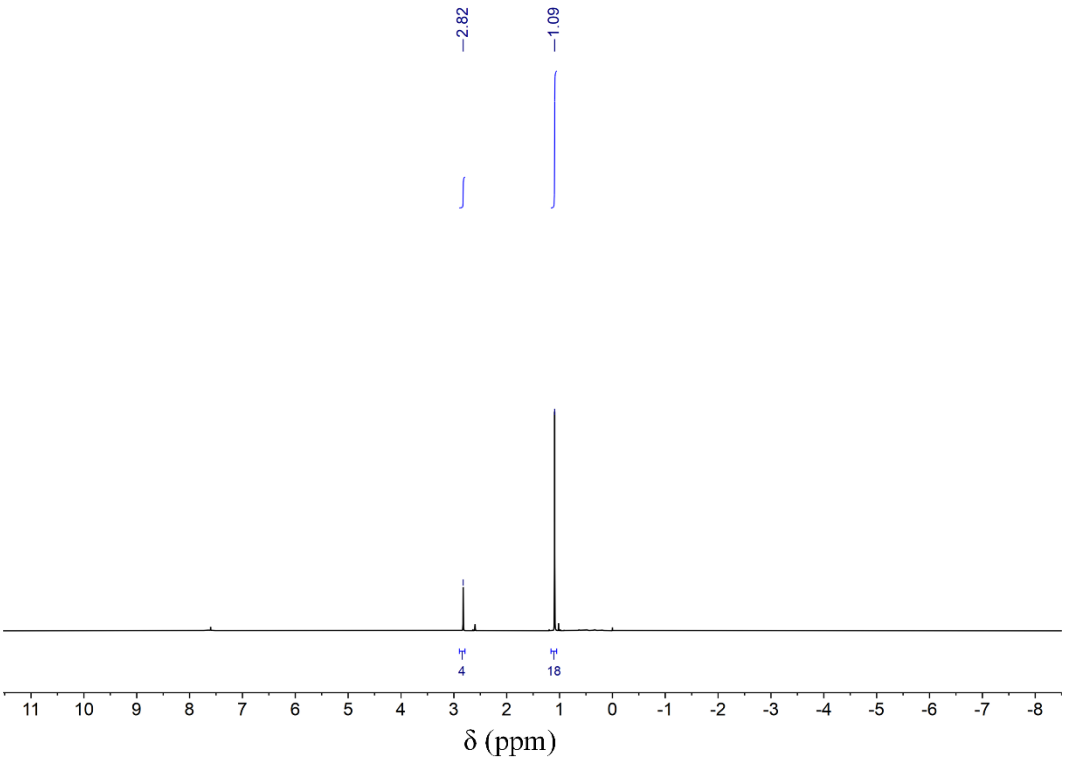

Figure S26. ^{1}H NMR of Dineopentylamine

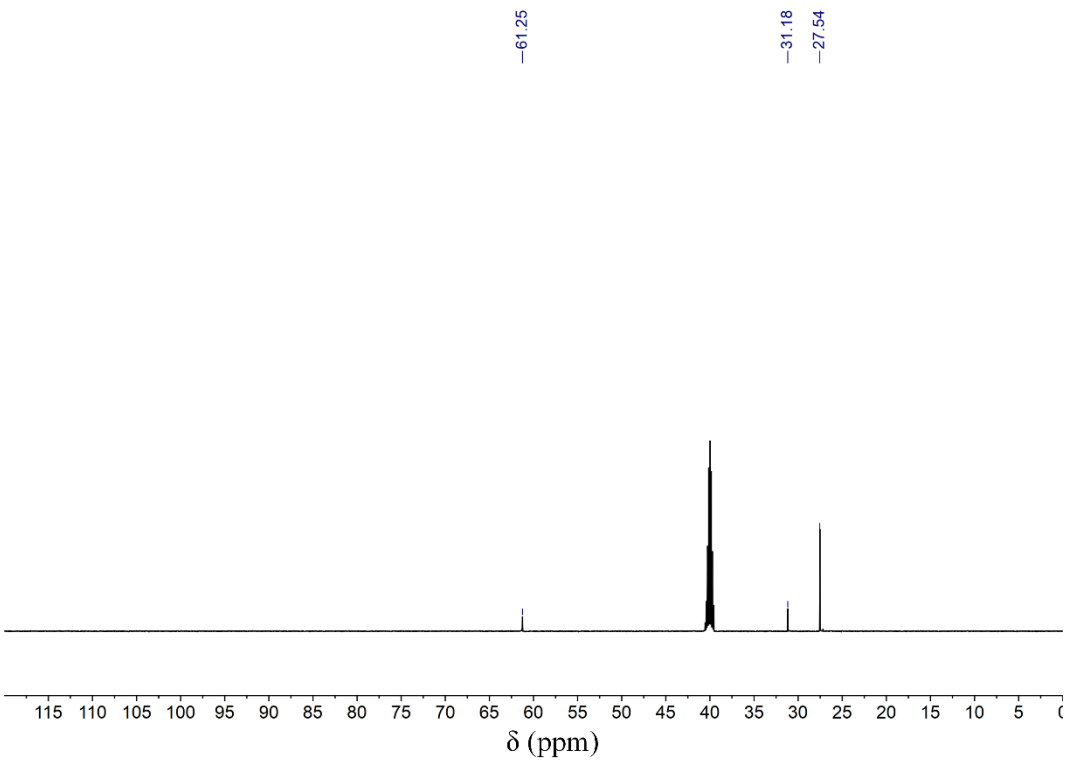

Figure S27. ^{13}C NMR of Dineopentylamine

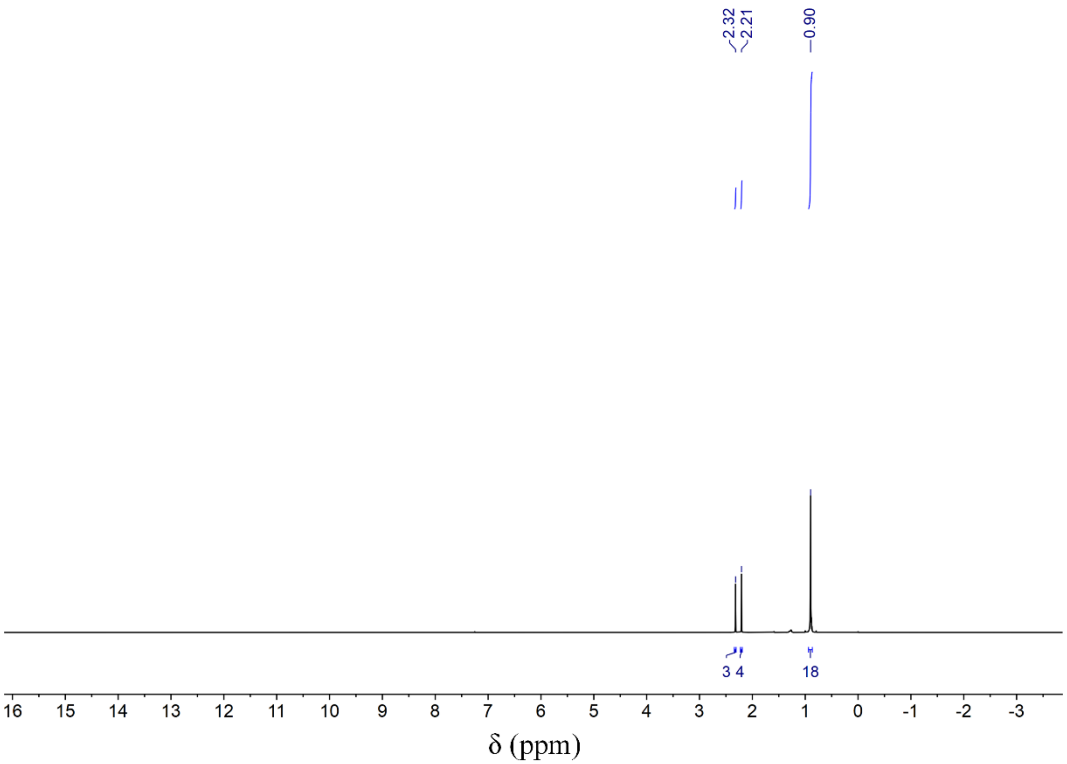

Figure S28. ^{1}H NMR of *N*,2,2-trimethyl-*N*-neopentylpropan-1-amine

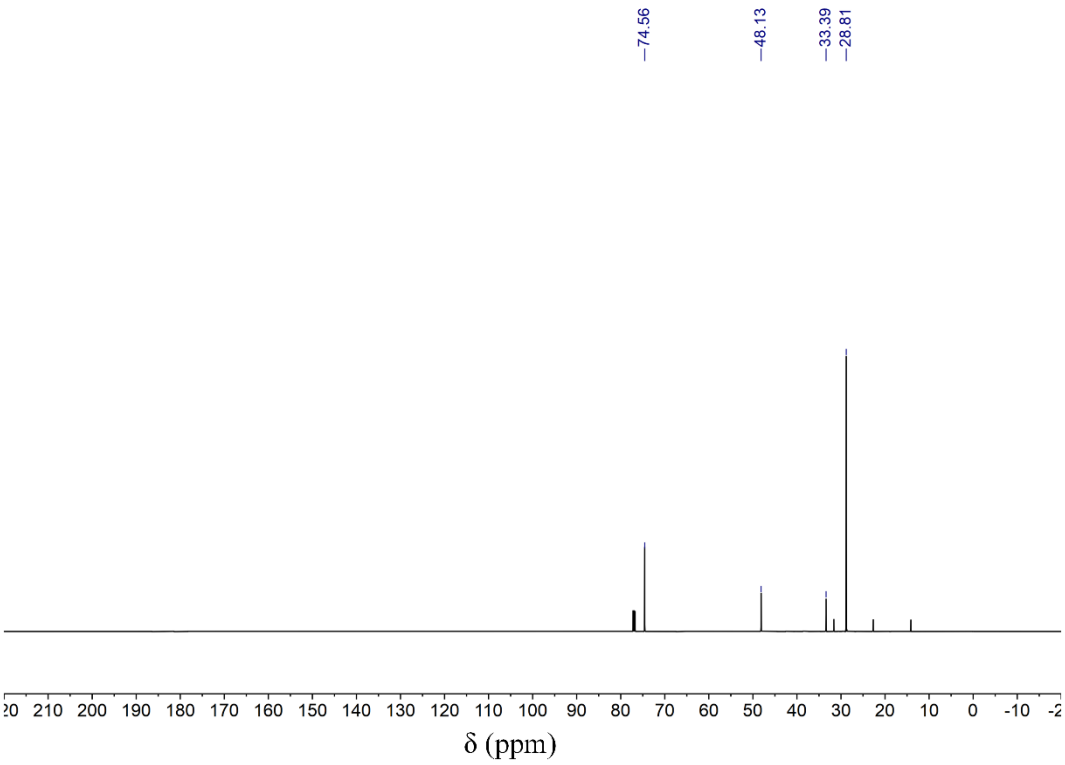

Figure S29. ^{13}C NMR of *N*,2,2-trimethyl-*N*-neopentylpropan-1-amine

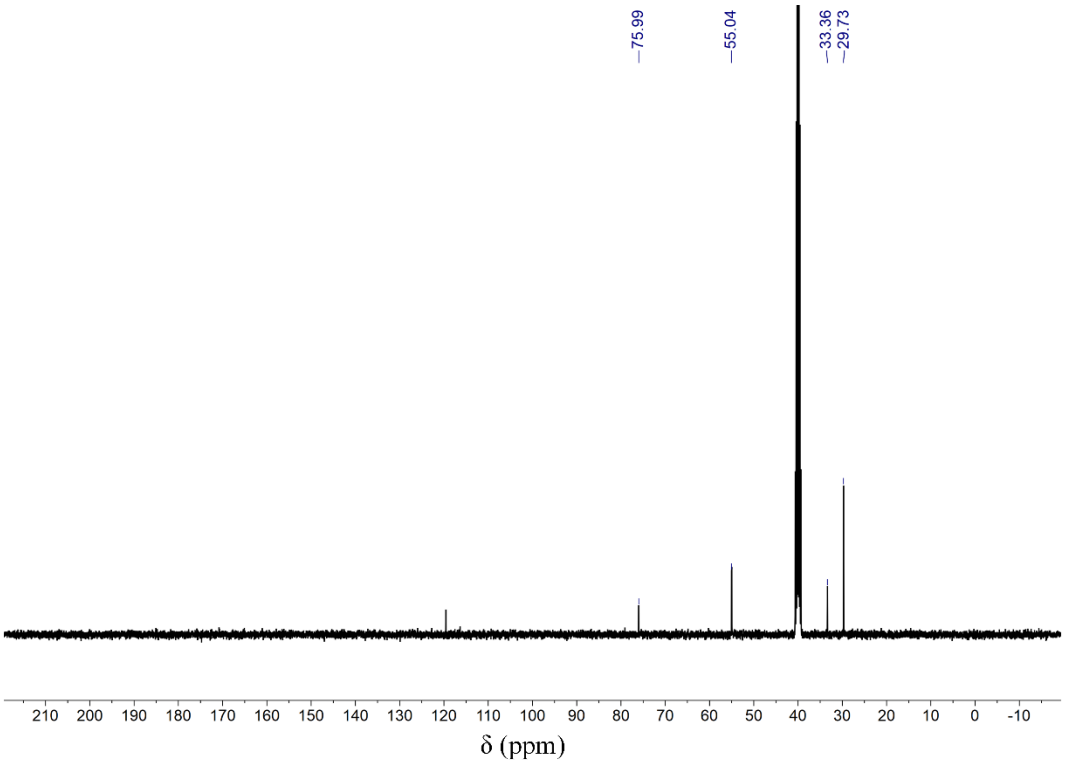

Figure S30. ^{1}H NMR of Dimethyldineopentylammonium fluoride

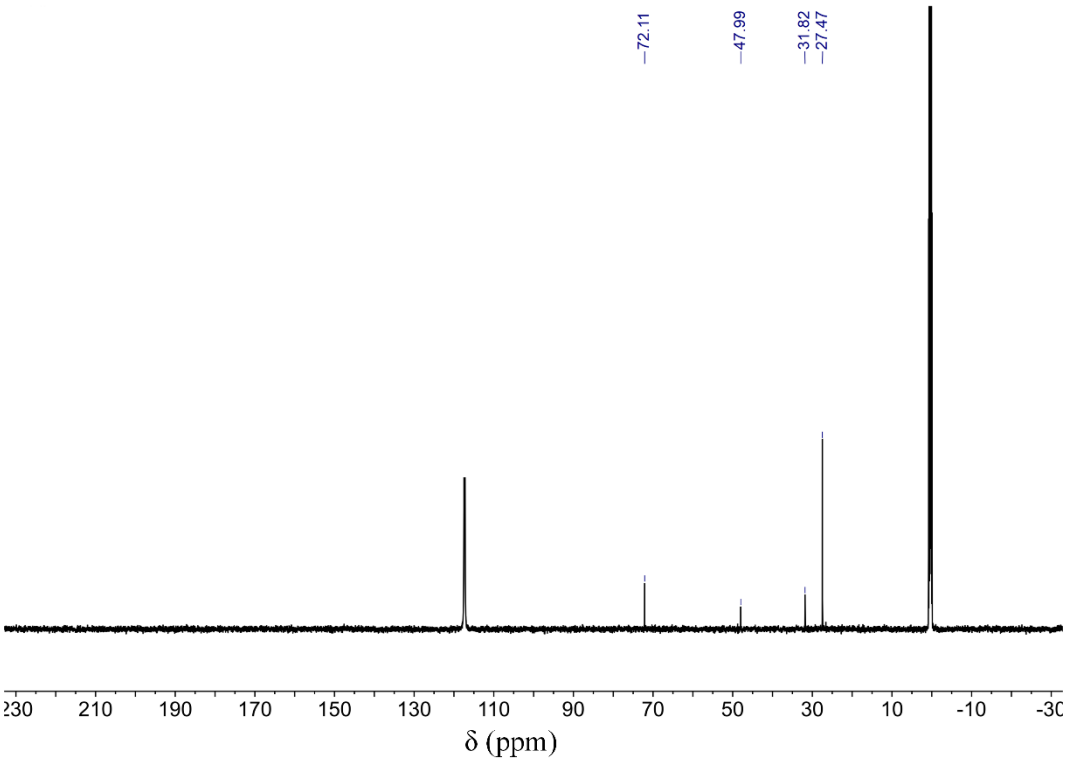

Figure S31. ^{13}C NMR of Dimethyldineopentylammonium fluoride

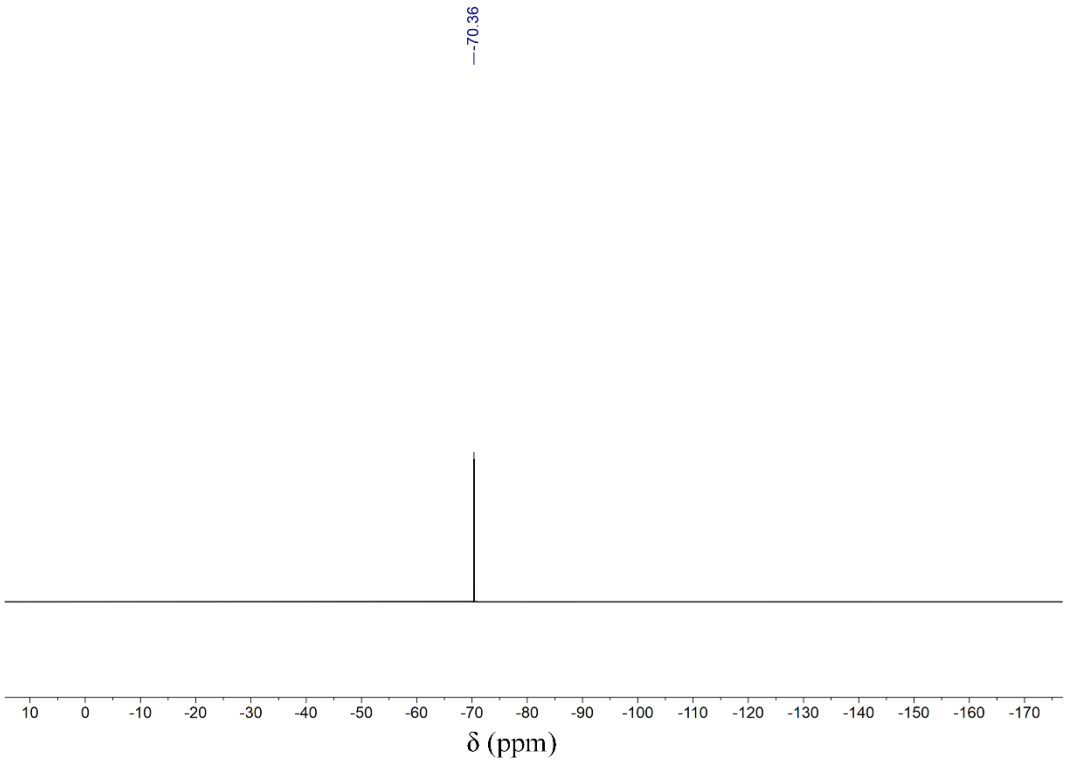

Figure S32. ^{19}F NMR of 1-(2-methoxyphenyl)-3-neopentyl-1*H*-imidazolium fluoride

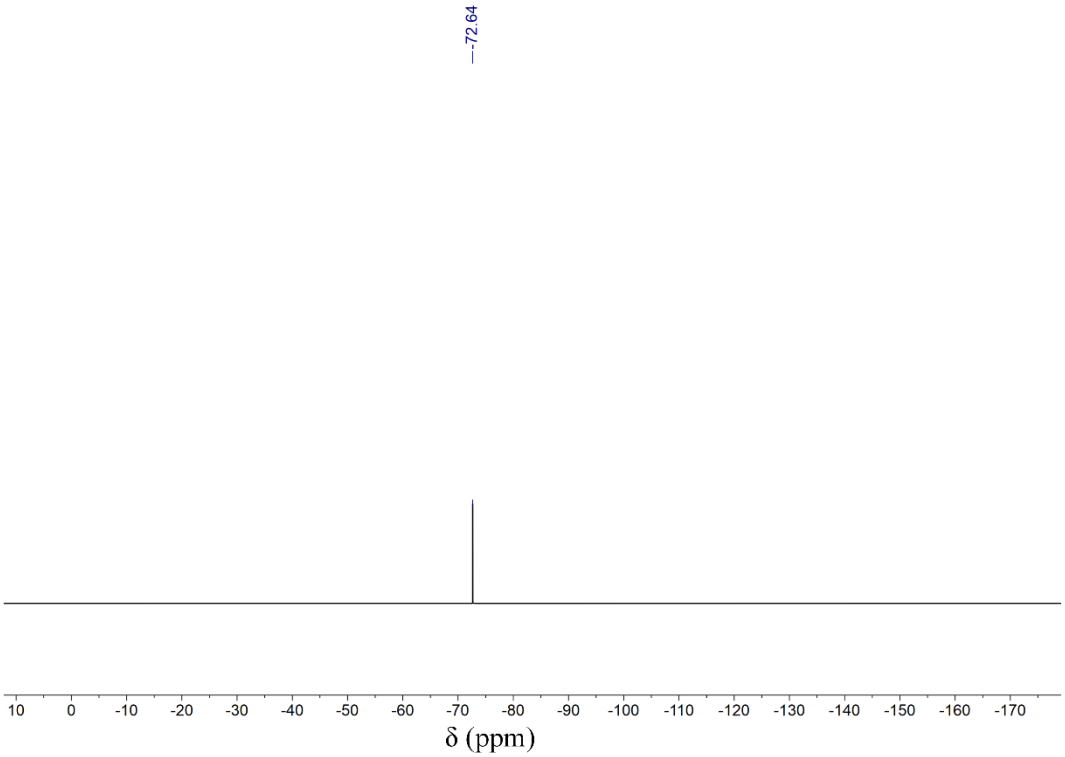

Figure S33. ^{19}F NMR of 1-(4-methoxyphenyl)-3-neopentyl-1*H*-imidazolium fluoride

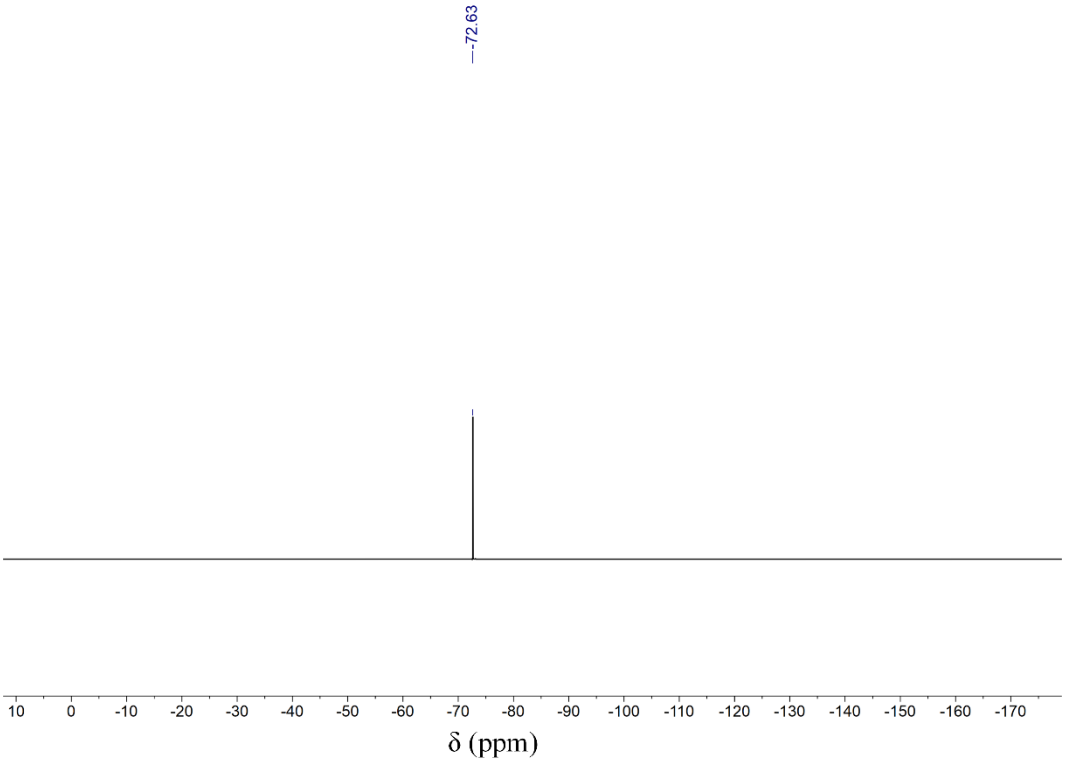

Figure S34. ^{19}F NMR of 3-neopentyl-1-(*o*-tolyl)-1*H*-imidazolium fluoride

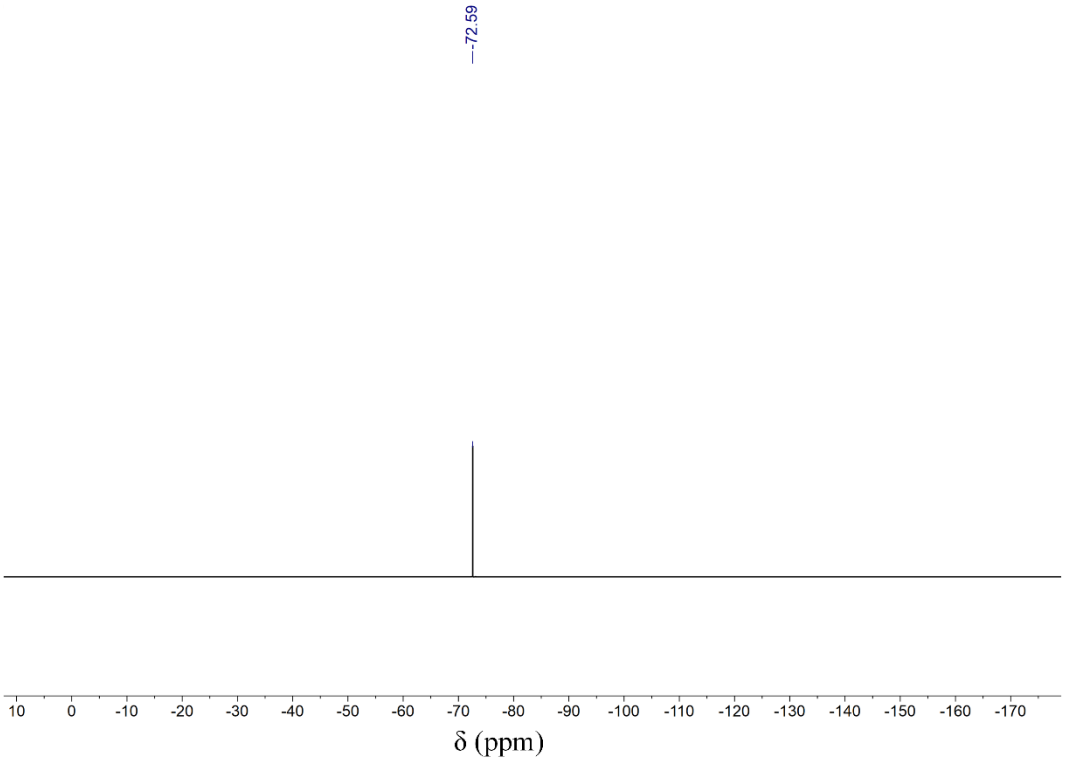

Figure S35. ^{19}F NMR of 3-neopentyl-1-(*p*-tolyl)-1*H*-imidazolium fluoride

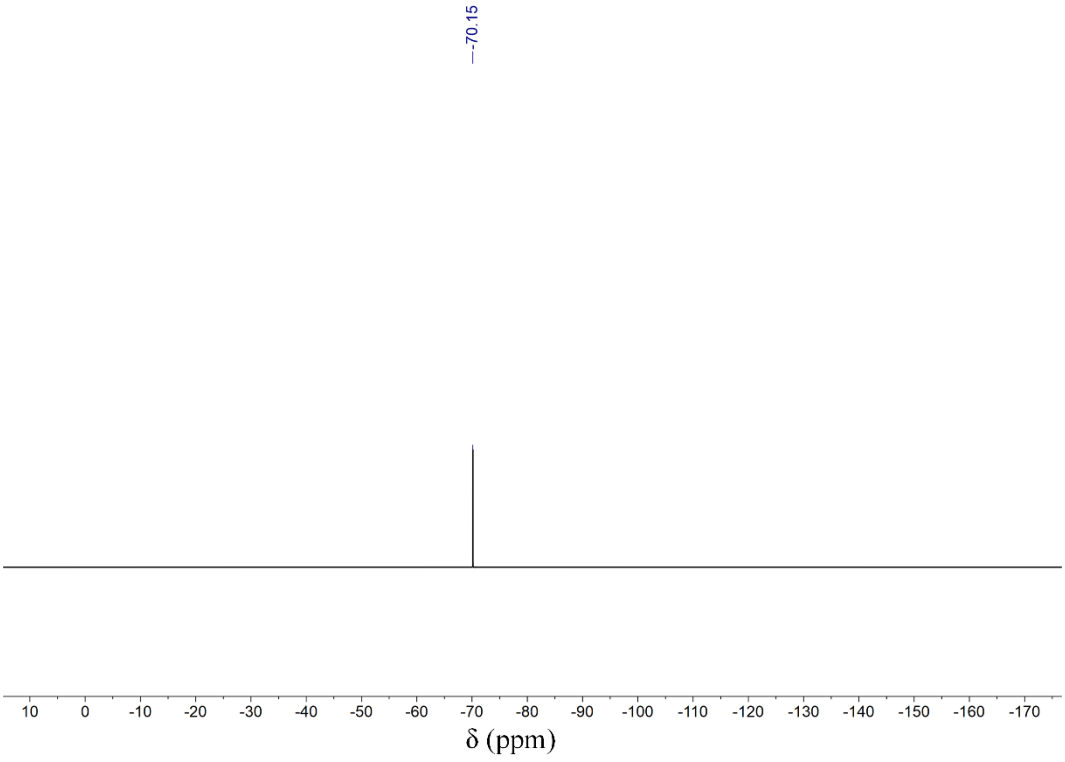

Figure S36. ^{19}F NMR of 1-(2,4-dimethoxyphenyl)-3-neopentyl-1*H*-imidazolium fluoride

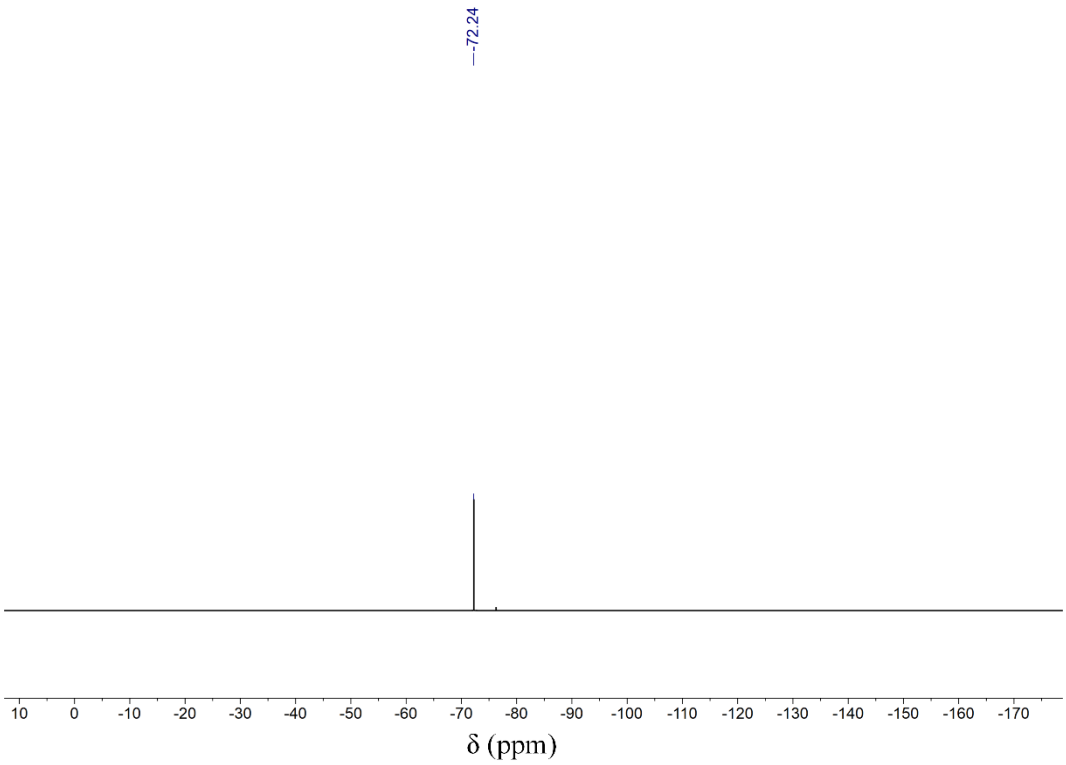

Figure S37. ^{19}F NMR of Trimethylneopentylammonium fluoride

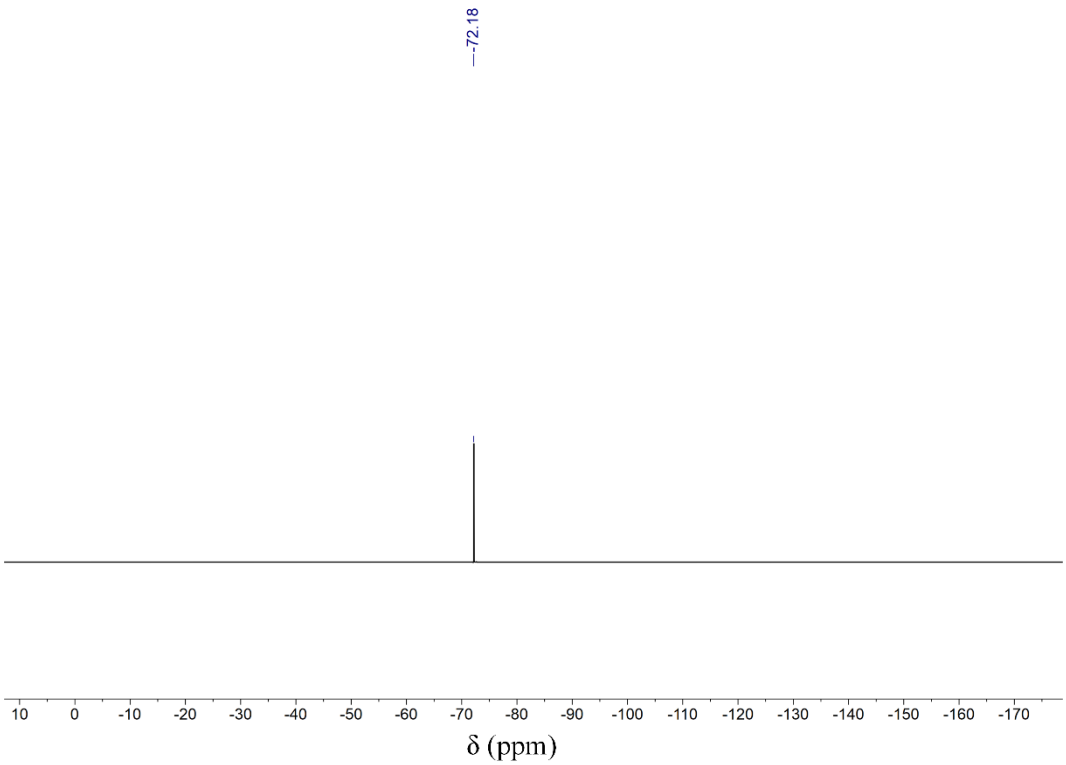

Figure S38. ^{19}F NMR of Dimethyldineopentylammonium fluoride

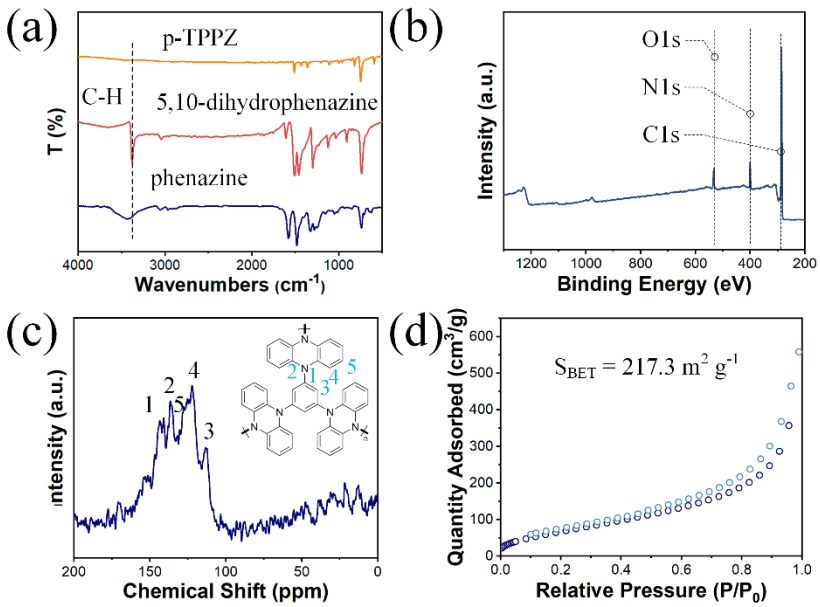

Figure S39. Characterizations of p-TPPZ. (a) FTIR spectra, (b) XPS spectra, (c) solid-state ^{13}C NMR spectra, and (d) N_2 adsorption–desorption isotherms.

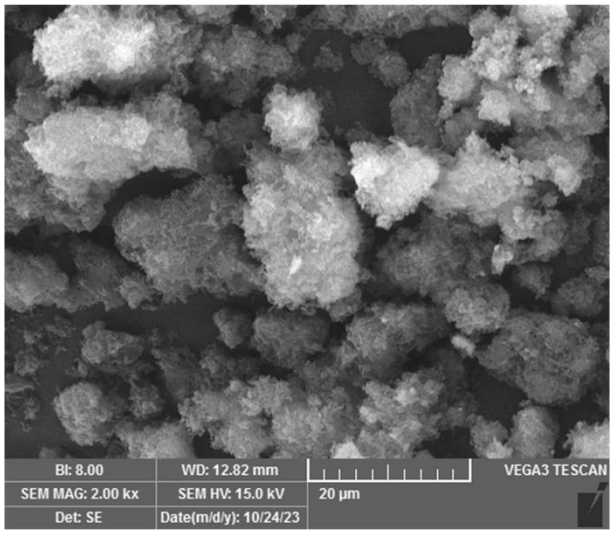

Figure S40. SEM image of p-TPPZ surface morphology.

Table S1. Energy of the model backbone group

Electrolyte	**Energy (Hartree)**	**Energy + $\frac{1}{2}F_2$ (Hartree)**
1	-769.1052	-868.8913
2	-769.1081	-868.8942
3	-693.8658	-793.6519
4	-693.8679	-793.6540
5	-883.6781	-983.4642
$Np_1^+F^-$	-371.6222	-471.4083
$Np_2^+F^-$	-528.9199	-628.7060
1/2 F_2	-99.7861	

Table S2. Binding energy between F^- and different binding sites of quaternary ammonium salts.

Electrolyte	Site ***i*** **(Hartree)**	Site ***ii*** **(Hartree)**	Site ***iii*** **(Hartree)**
1	-0.2341	-0.2296	-0.2324
2	-0.2541	-0.2541	-0.2541
3	-0.2541	-0.2542	-0.2542
4	-0.2544	-0.2360	-0.2544
5	-0.2338	-0.2276	-0.2330
$Np_1^+F^-$	-0.2476	-0.2351	-0.2491
$Np_2^+F^-$	-0.2470	-0.2317	-0.2470

Table S3. HOMO-LUMO gap of the most stable site.

Electrolyte	**HOMO**	**LOMO**	**Band Gap**
1 (Site ***i*****)**	-6.14 eV	-1.46 eV	4.68 eV
2 (Site ***i*****)**	-6.34 eV	-1.22 eV	5.12 eV
3 (Site ***ii*****)**	-7.07 eV	-1.12 eV	5.96 eV
4 (Site ***i*****)**	-6.75 eV	-1.34 eV	5.41 eV
5 (Site ***i*****)**	-6.13 eV	-1.27 eV	4.86 eV
$Np_1^+F^-$ (Site ***ii*****)**	-6.77 eV	0.46 eV	6.31 eV
$Np_2^+F^-$ (Site ***i*****)**	-6.70 eV	-0.48	6.22 eV

Table S4. Bonding orbital energy.

Electrolyte	**Binding orbital**	**Energy (Hartree)**
1 (Site ***i*****)**	71 (HOMO)	-0.2257
2 (Site ***i*****)**	70 (HOMO)	-0.2665
3 (Site ***ii*****)**	66 (HOMO)	-0.2639
4 (Site ***i*****)**	66 (HOMO)	-0.2667
5 (Site ***i*****)**	79 (HOMO)	-0.2253
$Np_1^+F^-$ (Site ***ii*****)**	42 (HOMO)	-0.2468
$Np_2^+F^-$ (Site ***i*****)**	58 (HOMO)	-0.2461

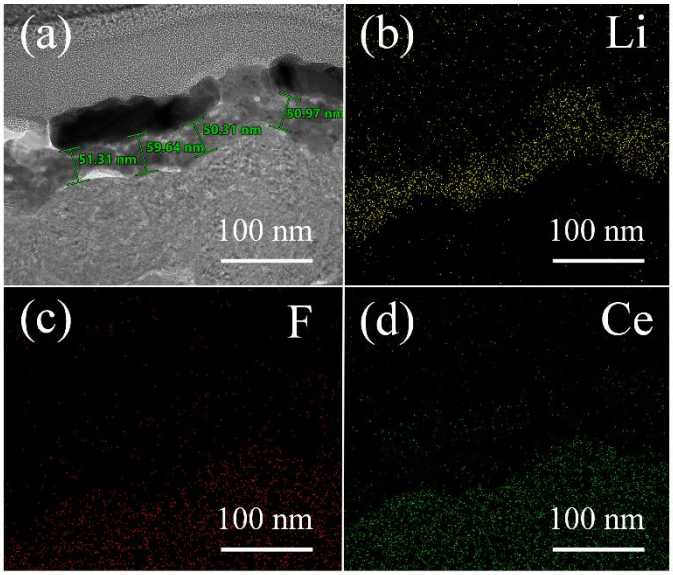

Figure S41. TEM images and corresponding EDS mapping of LiF–CeF_3 anode deposition morphologies.

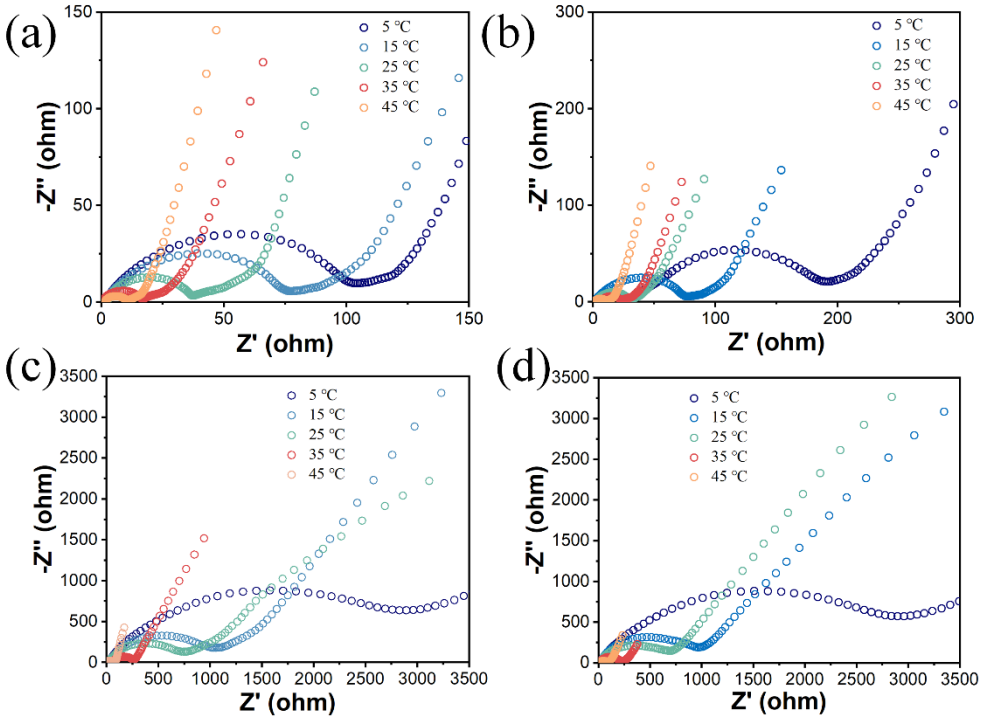

Figure S42. EIS measurements in a three-electrode cell at charged state with different Electrolytes and temperatures: (a)$D_5N^+F^-$, (b) $Np_2{}^+F^-$, (c) $D_5N^+HF_2^-$, and (d) $D_5N^+HF_2^-$.

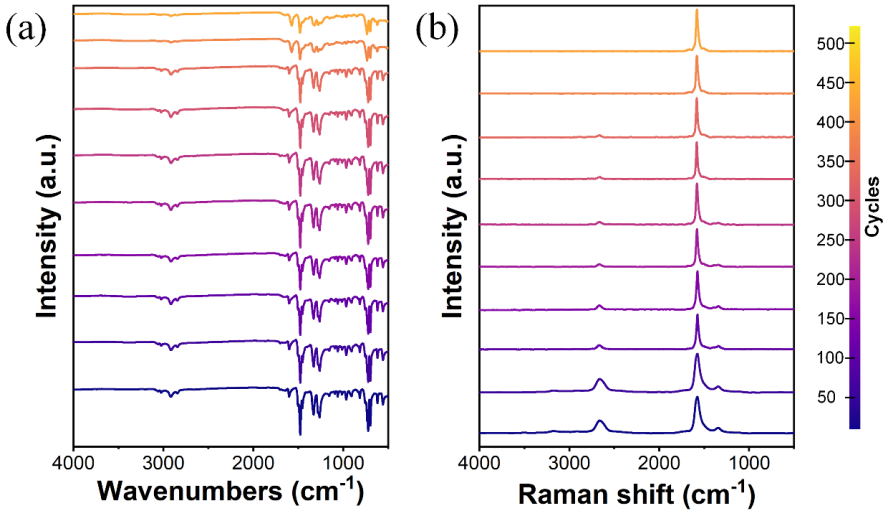

Figure S43. (a) Ex-situ FTIR spectrum and (b) Raman spectra of p-TPPZ under different charge/discharge states.

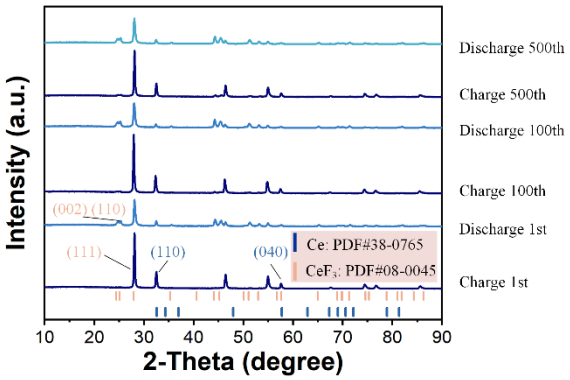

Figure S44. XRD of LiF–Ce under different charge/discharge states.

E. References

1. A. Modak, A. J. Nett, E. C. Swift, M. C. Haibach, V. S. Chan, T. S. Franczyk, S. Shekhar and S. P. Cook, *ACS Catal.*, 2020, **10**, 10495-10499.
2. J. Xiang, M. Chen, Y. Lei, J. Zhou, W. Zou, R. Lu and S. Zhang, *J. Mater. Chem. A.*, 2024, 2024, 12, 29493-29501.
3. S. Xu, H. Dai, S. Zhu, Y. Wu, M. Sun, Y. Chen, K. Fan, C. Zhang, C. Wang and W. Hu, *eScience*, 2021, **1**, 60-68.